References

[1] P. Abou-Sleiman, D. Healy, N. Quinn, N. Wood, The role of pathogenic *DJ-1* mutations in Parkinson's disease, Ann. Neurol. 54 (2003) 283–286.

[2] H. Aleyasin, M.W. Rousseaux, M. Phillips, R.H. Kim, R.J. Bland, S. Callaghan, R.S. Slack, M.J. During, T.W. Mak, D.S. Park, The Parkinson's disease gene DJ-1 is also a key regulator of stroke-induced damage, Proc. Natl. Acad. Sci. USA 104 (2007) 18748–18753.

[3] G. Annesi, G. Savettieri, P. Pugliese, M. D'Amelio, P. Tarantino, P. Ragonese, V. La Bella, T. Piccoli, D. Civitelli, F. Annesi, B. Fierro, F. Piccoli, G. Arabia, M. Caracciolo, I.C. Cirò Candiano, A. Quattrone, DJ-1 mutations and parkinsonism-dementia-amyotrophic lateral sclerosis complex, Ann. Neurol. 58 (2005) 803–807.

[4] V. Bonifati, P. Rizzu, M.J. van Baren, O. Schaap, G.J. Breedveld, E. Krieger, M.C. Dekker, F. Squitieri, P. Ibanez, M. Joosse, J.W. van Dongen, N. Vanacore, J.C. van Swieten, A. Brice, G. Meco, C.M. van Duijn, B.A. Oostra, P. Heutink, Mutations in the *DJ-1* gene associated with autosomal recessive early-onset parkinsonism, Science 299 (2003) 256–259.

[5] I.E. Clark, M.W. Dodson, C. Jiang, J.H. Cao, J.R. Huh, J.H. Seol, S.J. Yoo, B.A. Hay, M. Guo, Drosophila pink1 is required for mitochondrial function and interacts genetically with parkin, Nature 441 (2006) 1162–1166.

[6] L.N. Clark, S. Afridi, H. Mejia-Santana, J. Harris, E.D. Louis, L.J. Cote, H. Andrews, A. Singleton, F. Wavrant De-Vrieze, J. Hardy, R. Mayeux, S. Fahn, C. Waters, B. Ford, S. Frucht, R. Ottman, K. Marder, Analysis of an early-onset Parkinson's disease Cohort for *DJ-1* Mutations, Mov. Disord. 19 (2004) 796–800.

[7] A. Djarmati, K. Hedrich, M. Svetel, N. Schäfer, V. Juric, S. Vukosavic, R. Hering, O. Riess, S. Romac, C. Klein, V. Kostic, Detection of *Parkin* (*PARK2*) and *DJ1* (*PARK7*) mutations in early- onset Parkinson disease: *Parkin* mutation frequency depends on ethnic origin of patients, Hum. Mutat. 23 (2004) 525.

[8] M. Funayama, Y. Li, T.H. Tsoi, C.W. Lam, T. Ohi, S. Yazawa, E. Uyama, R. Djaldetti, E. Melamed, H. Yoshino, Y. Imamichi, H. Takashima, K. Nishioka, K. Sato, H. Tomiyama, S. Kubo, Y. Mizuno, N. Hattori, Familial parkinsonism with digenic parkin and PINK1 mutations, Mov. Disord. 23 (2008) 1461–1465.

[9] S. Hague, E. Rogaeva, D. Hernandez, C. Gulick, A. Singleton, M. Hanson, J. Johnson, R. Weiser, M. Gallardo, B. Ravina, K. Gwinn-Hardy, A. Crawley, P. St George-Hyslop, A. Lang, P. Heutink, V. Bonifati, J. Hardy, A. Singleton, Early-onset Parkinson's disease caused by a compound heterozygous *DJ-1* mutation, Ann. Neurol. 54 (2003) 271–274.

[10] M. Hasegawa, T. Arai, H. Akiyama, T. Nonaka, H. Mori, T. Hashimoto, M. Yamazaki, K. Oyanagi, TDP-43 is deposited in the Guam parkinsonism-dementia complex brains, Brain 130 (2007) 1386–1394.

[11] Y. Hatano, Y. Li, K. Sato, S. Asakawa, Y. Yamamura, H. Tomiyama, H. Yoshino, M. Asahina, S. Kobayashi, S. Hassin-Baer, C.S. Lu, A.R. Ng, R.L. Rosales, N. Shimizu, T. Toda, Y. Mizuno, N. Hattori, Novel *PINK1* mutations in early-onset parkinsonism, Ann. Neurol. 56 (2004) 424–427, Erratum in: Ann. Neurol. 56 (2004) 603.

[12] K. Hedrich, A. Djarmati, N. Schäfer, R. Hering, C. Wellenbrock, P. Weiss, R. Hilker, P. Vieregge, L. Ozelius, P. Heutink, V. Bonifati, E. Schwinger, A. Lang, J. Noth, S. Bressman, P. Pramstaller, O. Riess, C. Klein, *DJ-1 (PARK7)* mutations are less frequent than *Parkin (PARK2)* mutations in early-onset Parkinson disease, Neurology 62 (2004) 389–394.

[13] K. Hedrich, N. Schäfer, R. Hering, J. Hagenah, A. Lanthaler, E. Schwinger, P. Kramer, L. Ozelius, S. Bressman, G. Abbruzzese, P. Martinelli, V. Kostic, P. Pramstaller, P. Vieregge, O. Riess, C. Klein, The R98Q variation in DJ-1 represents a rare polymorphism, Ann. Neurol. 55 (2004) 145.

[14] P. Ibáñez, G. Michele, V Bonifati, E Lohmann, S. Thobois, P Pollak, Y. Agid, P Heutink, A Dürr, A. Brice, French Parkinson's Disease Genetics Study Group, Screening for DJ-1 mutations in early onset autosomal recessive parkinsonism, Neurology 61 (2003) 1429–1431.

[15] P. Jenner, Oxidative stress in Parkinson's disease, Ann. Neurol. 53 (suppl. 3) (2003) S26–S38.

[16] T. Kitada, S. Asakawa, N. Hattori, H. Matsumine, Y. Yamamura, S. Minoshima, M. Yokochi, Y. Mizuno, N. Shimizu, Mutations in the *parkin* gene cause autosomal recessive juvenile parkinsonism, Nature 392 (1998) 605–608.

[17] R. Kumazawa, H. Tomiyama, Y. Li, Y. Imamichi, M. Funayama, H. Yoshino, F. Yokochi, T. Fukusako, Y. Takehisa, K. Kashihara, T. Kondo, B. Elibol, S. Bostantjopoulou, T. Toda, H. Takahashi, F. Yoshii, Y. Mizuno, N. Hattori, Mutation analysis of the PINK1 gene in 391 patients with Parkinson's disease, Arch. Neurol. 65 (2008) 802–808.

[18] S. Kuzuhara, Y. Kokubo, R. Sasaki, Y. Narita, T. Yabana, M. Hasegawa, T. Iwatsubo, Familial amyotrophic lateral sclerosis and parkinsonism-dementia complex of the Kii Peninsula of Japan: clinical and neuropathological study and tau analysis, Ann. Neurol. 49 (2001) 501–511.

[19] Y. Li, H. Tomiyama, K. Sato, Y. Hatano, H. Yoshino, M. Atsumi, M. Kitaguchi, S. Sasaki, S. Kawaguchi, H. Miyajima, T. Toda, Y. Mizuno, N. Hattori, Clinicogenetic study of PINK1 mutations in autosomal recessive early-onset parkinsonism, Neurology 64 (2005) 1955–1957.

[20] C.B. Lücking, A. Dürr, V. Bonifati, J. Vaughan, G. De Michele, T. Gasser, B.S. Harhangi, G. Meco, P. Denèfle, N.W. Wood, Y. Agid, A. Brice, French Parkinson's Disease Genetics Study Group, European consortium on genetic susceptibility in Parkinson's disease. Association between early-onset Parkinson's disease and mutations in the parkin gene, N. Engl. J. Med. 342 (2000) 1560–1567.

[21] D. Nagakubo, T. Taira, H. Kitaura, M. Ikeda, K. Tamai, S.M. Iguchi-Ariga, H. Ariga, DJ-1, a novel oncogene which transforms mouse NIH3T3 cells in cooperation with ras, Biochem. Biophys. Res. Commun. 231 (1997) 509–513.

[22] M. Neumann, D. Sampathu, L. Kwong, A. Truax, M. Micsenyi, T. Chou, J. Bruce, T. Schuck, M. Grossman, C. Clark, L. McCluskey, B. Miller, E. Masliah, I. Mackenzie, H. Feldman, W. Feiden, H. Kretzschmar, J. Trojanowski, V. Lee, Ubiquitinated TDP-43 in frontotemporal lobar degeneration and amyotrophic lateral sclerosis, Science 314 (2006) 130–133.

[23] Y.P. Ning, K. Kanai, H. Tomiyama, Y. Li, M. Funayama, H. Yoshino, S. Sato, M. Asahina, S. Kuwabara, A. Takeda, T. Hattori, Y. Mizuno, N. Hattori, *PARK9*-linked parkinsonism in Eastern Asia: mutation detection in *ATP13A2* and clinical phenotype, Neurology 7 (2008) 1491–1493.

[24] J. Park, S.B. Lee, S. Lee, Y. Kim, S. Song, S. Kim, E. Bae, J. Kim, M. Shong, J.M. Kim, J. Chung, Mitochondrial dysfunction in Drosophila PINK1 mutants is complemented by parkin, Nature 441 (2006) 1157–1161.

[25] A. Ramirez, A. Heimbach, J. Grundemann, B. Stiller, D. Hampshire, L.P. Cid, I. Goebel, A.F. Mubaidin, A.L. Wriekat, J. Roeper, A. Al-Din, A.M. Hillmer, M. Karsak, B. Liss, C.G. Woods, M.I. Behrens, C. Kubisch, Hereditary parkinsonism with dementia is caused by mutations in ATP13A2, encoding a lysosomal type 5 p-type ATPase, Nat. Genet. 38 (2006) 1184–1191.

[26] P. Rizzu, D.A. Hinkle, V. Zhukareva, V. Bonifati, L.A. Severijnen, D. Martinez, R. Ravid, W. Kamphorst, J.H. Eberwine, V.M. Lee, J.Q. Trojanowski, P. Heutink, DJ-1 colocalizes with tau inclusions: a link between parkinsonism and dementia, Ann. Neurol. 55 (2004) 113–118.

[27] J. Sreedharan, J. Sreedharan, I.P. Blair, V.B. Tripathi, X. Hu, C. Vance, B. Rogelj, S. Ackerley, J.C. Durnall, K.L. Williams, E. Buratti, F. Baralle, J. de Belleroche, J.D. Mitchell, P.N. Leigh, A. Al-Chalabi, C.C. Miller, G. Nicholson, C.E. Shaw, TDP-43 mutations in familial and sporadic amyotrophic lateral sclerosis, Science 319 (2008) 1668–1672.

[28] B. Tang, H. Xiong, P. Sun, Y. Zhang, D. Wang, Z. Hu, Z. Zhu, H. Ma, Q. Pan, J.H. Xia, K. Xia, Z. Zhang, Association of PINK1 and DJ-1 confers digenic inheritance of early-onset Parkinson's disease, Hum. Mol. Genet. 15 (2006) 1816–1825.

[29] H. Tomiyama, Y. Kokubo, R. Sasaki, Y. Li, Y. Imamichi, M. Funayama, Y. Mizuno, N. Hattori, S. Kuzuhara, Mutation analyses in amyotrophic lateral sclerosis/parkinsonism-dementia complex of the Kii peninsula, Japan Mov. Disord. 23 (2008) 2344–2348.

[30] E.M. Valente, P.M. Abou-Sleiman, V. Caputo, M.M. Muqit, K. Harvey, S. Gispert, Z. Ali, D. Del Turco, A.R. Bentivoglio, D.G. Healy, A. Albanese, R. Nussbaum, R. González-Maldonado, T. Deller, S. Salvi, P. Cortelli, W.P. Gilks, D.S. Latchman, R.J. Harvey, B. Dallapiccola, G. Auburger, N.W. Wood, Hereditary early-onset Parkinson's disease caused by mutations in *PINK1*, Science 304 (2004) 1158–1160.

[31] E.M. Valente, S. Salvi, T. Ialongo, R. Marongiu, A.E. Elia, V. Caputo, L. Romito, A. Albanese, B. Dallapiccola, A.R. Bentivoglio, PINK1 mutations are associated with sporadic early-onset parkinsonism, Ann. Neurol. 56 (2004) 336–341.

[32] C. van Duijn, M. Dekker, V. Bonifati, R. Galjaard, J. Houwing-Duistermaat, P. Snijders, L. Testers, G. Breedveld, M. Horstink, L. Sandkuijl, J. van Swieten, B. Oostra, P. Heutink, PARK7, a novel locus for autosomal recessive early-onset parkinsonism, on chromosome 1p36, Am. J. Hum. Genet. 69 (2001) 629–634.

FEBS Letters 583 (2009) 2194–2200

FEBS Letters

journal homepage: www.FEBSLetters.org

Excitatory amino acid transporter 2 associates with phosphorylated tau and is localized in neurofibrillary tangles of tauopathic brains

Kumi Sasaki [a,b], Hideki Shimura [a,b], Masako Itaya [c], Ryota Tanaka [a], Hideo Mori [d], Yoshikuni Mizuno [d], Kenneth S. Kosik [e], Shigeki Tanaka [a], Nobutaka Hattori [c,*]

[a] Department of Neurology, Juntendo University Urayasu Hospital, Japan
[b] Institute for Environment and Gender Specific Medicine, Japan
[c] Juntendo University School of Medicine, Japan
[d] Juntendo University Koshigaya Hospital, Japan
[e] Neuroscience Research Institute, University of California, USA

ARTICLE INFO

Article history:
Received 7 May 2009
Revised 2 June 2009
Accepted 5 June 2009
Available online 13 June 2009

Edited by Jesus Avila

Keywords:
Alzheimer's disease
Progressive supranuclear palsy
Corticobasal degeneration
EAAT2
Tau
Neurofibrillary tangle

ABSTRACT

Phosphorylated tau (p-tau) is the principal component of neurofibrillary tangles, a pathological hallmark, and likely plays a neurotoxic role in tauopathies including Alzheimer's disease (AD), progressive supranuclear palsy (PSP), and corticobasal degeneration (CBD). We subjected brains from autopsy cases of AD, PSP, and CBD to a variety of immunohistochemical, immunoblotting, and pull-down assays. In this study, we show that excitatory amino acid transporter 2 (EAAT2) preferentially interacted with phosphorylated tau and was localized in neurofibrillary tangles in the brains of such patients. These results strongly indicate that EAAT2 acts in tauopathy-related neurodegeneration, and abnormalities in glutamate transport play an important role in the pathogenesis of tauopathies.

Structured summary:
MINT-7148349, MINT-7148361:*TAU* (uniprotkb:P10636) *physically interacts* (MI:0914) with *EAAT2* (uniprotkb:P43004) by *pull-down* (MI:0096)
MINT-7148372, MINT-7148384:*TAU* (uniprotkb:P10636) *physically interacts* (MI:0914) with *EAAT2* (uniprotkb:P43004) by *anti bait coimmunoprecipitation* (MI:0006)

1. Introduction

Tau is a microtubule-associated protein mainly expressed in neurons where it plays a role in the assembly and stability of the microtubule network. Tau is also strongly linked to several neurodegenerative disorders as the principle pathological component of filamentous inclusions called neurofibrillary tangles (NFTs) found in the brains of Alzheimer's disease (AD) patients and in a variety of diseases collectively called "tauopathies", including progressive supranuclear palsy (PSP) and corticobasal degeneration (CBD) [1]. Although these diseases are sporadic, the tau gene can harbor mutations leading to diverse clinical phenotypes collectively grouped under frontotemporal dementia with parkinsonism linked to chromosome 17 [2].

Phosphorylated tau (p-tau) has been identified as a major protein component of NFTs [3,4]. Considerable evidence supports that p-tau represents the pathological entity in tauopathies, including the observation that increased p-tau causes neuronal cell death [5]. Because phosphorylation releases tau from microtubules and tau in NFTs is phosphorylated, kinases have been viewed suspiciously for a possible pathogenetic role. In vivo evidence for interaction with tau exists for cyclin-dependent kinase-5 (cdk5)/p25 and glycogen synthase kinase-3β (GSK-3β). Tau phosphorylation by cdk5 in mice [6] and GSK-3β in flies [7] can cause or accelerate NFT formation in vivo with an attendant worsening of neurodegeneration. Moreover, as endogenous tau was phosphorylated, aggregated tau accumulated, and neurofibrillary pathology developed progressively in these animals.

In light of such evidence, analyzing the molecular complex of p-tau and mechanism of p-tau-induced cell death is important for

Abbreviations: AD, Alzheimer's disease; PSP, progressive supranuclear palsy; CBD, corticobasal degeneration; EAAT2, excitatory amino acid transporter 2; NFTs, neurofibrillary tangles; GSK-3β, glycogen synthase kinase-3β; p-tau, phosphorylated tau; GLT1, glutamate transporter

* Corresponding author. Address: Department of Neurology, Juntendo University School of Medicine, 2-1-1 Hongo, Bunkyo, Tokyo 113-8421, Japan. Fax: +81 3 58000547.
E-mail address: nhattori@juntendo.ac.jp (N. Hattori).

0014-5793/$36.00 © 2009 Federation of European Biochemical Societies. Published by Elsevier B.V. All rights reserved.
doi:10.1016/j.febslet.2009.06.015

understanding the pathogenesis of tauopathies. In previous studies, we showed that CHIP and HSP27 interact with p-tau, decrease its amounts, and protect against p-tau-induced neurotoxicity [8,9]. In this study, we provide evidence that excitatory amino acid transporter 2 (EAAT2) is a molecular complex of p-tau. EAAT2 is a glutamate transporter and its dysfunction is tightly linked to neurodegenerative disorders [10]. We also demonstrate that EAAT2 preferentially interacts with p-tau rather than dephosphorylated tau and is localized within NFTs of patients with AD, PSP, and CBD.

2. Materials and methods

2.1. Antibodies

The EAAT2 polyclonal antibody, also known as HS5, which is an antibody to the 20-mer sequence (TEGANNMPKQVEVRNHDSHL) at the N-terminal domain of human EAAT2, was generated and characterized as described previously [11]. The anti-tau antibodies used included tau antibodies, anti-phosphorylated tau antibodies, and anti-non-phosphorylated tau antibodies. The tau antibody used was a monoclonal mouse tau antibody (Sigma, St. Louis, MO, USA), which recognizes all tau isoforms. The anti-phosphorylated tau antibodies used included AT8 (Pierce, Rockford, IL, USA), which recognizes phosphorylated S202 and T205 residues, and PHF1 [12,13], which recognizes phosphorylated S396 and S404 residues. Tau 1 [14] was used as an anti-non-phosphorylated tau antibody, which recognizes non-phosphorylated S199, S202, and T205 residues. Rabbit anti-EAAT2 antibody H85 and goat anti-EAAT2 antibody N19 were obtained from Santa Cruz Biotechnology, Inc., Santa Cruz, CA, USA.

Table 1
Clinical data of all autopsied subjects.

Case	Age	Sex	Postmortem delay (h)
Normal 1	66	Male	5
Normal 2	70	Female	2.5
Normal 3	81	Male	2.5
AD1	66	Male	3.5
AD2	72	Female	3
AD3	76	Male	5
AD4	81	Female	4.5
PSP1	69	Male	6.5
PSP2	85	Female	3.5
CBD1	61	Male	8
CBD2	81	Female	9

2.2. In vitro phosphorylation

Active recombinant GSK-3β (Upstate Biotechnology, Lake Placid, NY, USA) and Cdk5/p25 (Cosmo Bio Co. Ltd., Tokyo, Japan) were incubated in a reaction mixture containing 2 mM ATP, 20 mM HEPES (pH 6.8), 10 mM $MgCl_2$, and 10 mM $MnCl_2$ with recombinant His-tau (Sigma). Tau phosphorylation sites were confirmed by the phosphorylated tau-specific antibodies PHF1 (S396 and S404) and AT8 (S202 and T205).

2.3. Brain tissue samples

Brain tissue was obtained by autopsy from four AD (AD1, 2, 3 and 4), two CBD (CBD1 and 2), two PSP (PSP1 and 2), and three normal cases (normal 1, 2 and 3). Autopsies were performed by authorized pathologists to confirm diagnosis or other clinical imperatives. Informed consent was obtained from the next-of-kin in all cases. Diagnoses were performed by viewing the pathological sections. Age, sex, and postmortem delay are summarized in Table 1.

2.4. Immunopurification and immunoblotting

Immunopurification, immunoblotting, and pull-down assays were performed as described previously [8,9]. Temporal cortex specimens (2 g) were homogenized in lysis buffer containing 1% Triton-X 100 and sedimented at 20 000×*g* for 1 h at 4 °C. Supernatants were incubated with protein A/G (Pierce) bound to the tau monoclonal antibody (Sigma) or HS5 for 2 h at 4 °C. SDS buffer (4×) was added to lysates and immunoprecipitates. SDS–PAGE and immunoblotting were performed as described previously [11,12]. The intensity was analyzed using a chemiluminescence image analyzer Las-1000 Plus (Fuji film, Tokyo, Japan). The value was compared to that of AD1.

2.5. Pull-down assays

Either His-tau or phosphorylated His-tau-coupled nickel beads were added to human brain homogenates incubated at 4 °C for 1 h with shaking. We added 4× SDS to release precipitated proteins from the beads. The eluted fraction was transferred to a new tube after centrifugation and 0.1 N Tris–HCl buffer (pH 8.5) was added.

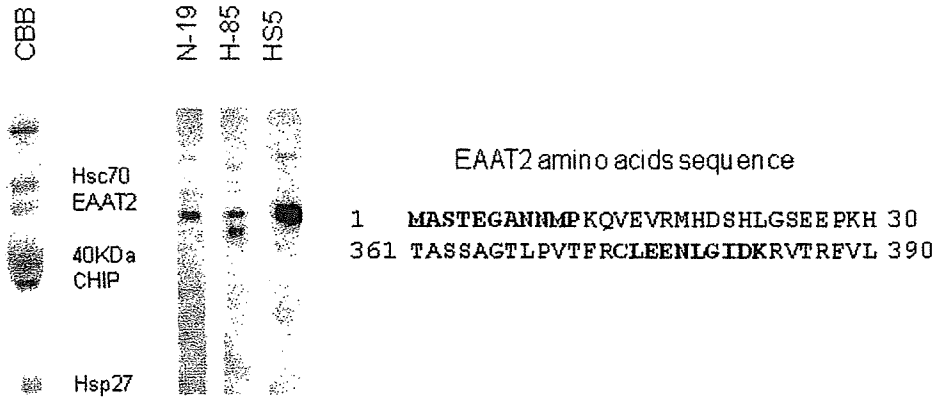

Fig. 1. Excitatory amino acid transporter 2 (EAAT2) interacts with phosphorylated tau. Human brain homogenates were passed over nickel beads coupled to His-tau that had been phosphorylated by GSK-3β and Cdk5/p25. Eluates were separated by SDS–PAGE and stained with Coomassie brilliant blue (CBB) or immunoblotted with antibodies to EAAT2. The peptide sequence (bold) obtained from the 62-kDa band was consistent with the human EAAT2 protein sequence (NCB Accession # NP 004162).

2.6. Immunohistochemistry

Immunohistochemical studies were performed as described previously [13]. Sections (10-μm thick) of formalin-fixed, paraffin-embedded tissue from the medial temporal cortex were incubated with 70% formic acid for antigen activation followed by immunostaining with EAAT2 antibodies. By confocal microscopy, AT8 (Pierce), which specifically recognizes p-tau, was visualized by a secondary antibody conjugated to Texas Red and EAAT2 by a secondary antibody conjugated to FITC.

2.7. Extraction of sarkosyl-insoluble proteins

Sarkosyl-insoluble proteins were extracted from the temporal cortex as described previously [14]. Extracts were divided into

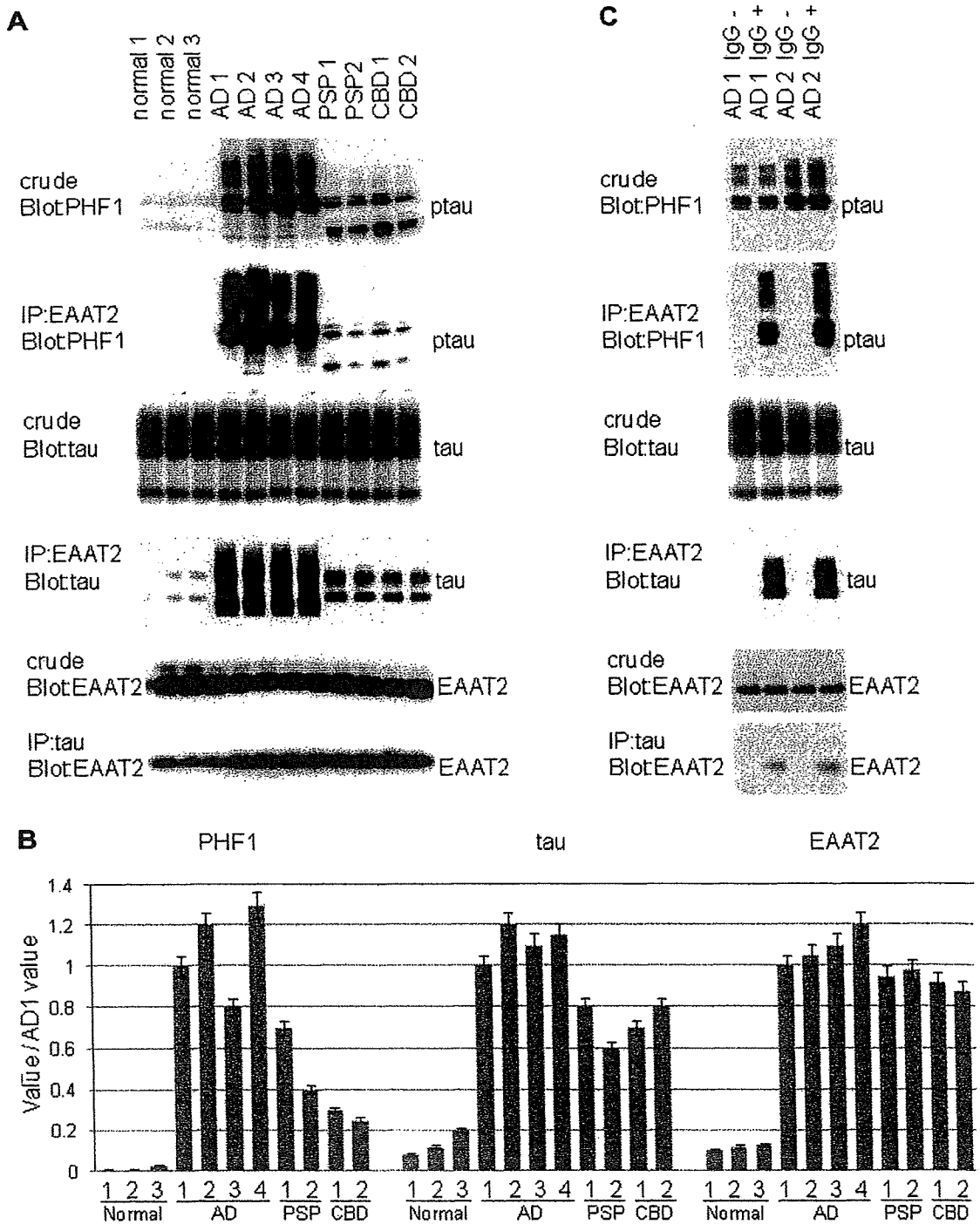

Fig. 2. (A) Brain homogenates of the temporal cortex from four Alzheimer's disease (AD), two progressive supranuclear palsy (PSP), two corticobasal degeneration (CBD), and three normal cases were immunoprecipitated with HS5 polyclonal EAAT2 or monoclonal tau antibodies. Precipitates were analyzed by PHF1, monoclonal tau, or HS5 polyclonal EAAT2 antibodies. (B) Quantitative analysis of immunoprecipitated tau and EAAT2 levels standardized against the amount of protein detected in relevant crude homogenates. Values are normalized to the value of AD1. Data are presented as mean S.D. (C) Analysis of antibody specificity for immunoprecipitation.

TBS-soluble, 1% Triton-X 100-soluble, sarkosyl-soluble, and sarkosyl-insoluble fractions.

3. Results

We sought to identify molecular complexes associated with tau when it is phosphorylated at sites that are phosphorylated in AD (Ser-202, Thr-205, Ser-396, and Ser-404). Human brain homogenates were passed through an affinity column with nickel beads coupled to a recombinant four-repeat His-tau phosphorylated by Cdk5/p25 and GSK-3β, and associated proteins were eluted with 1 M NaCl. Eluted proteins were separated by SDS–PAGE and several bands were stained with Coomassie Brilliant Blue (CBB). A 62-kDa CBB band was identified by mass spectrometry that contained the sequences MASTEGANNMP and CLEENLGIDK, which exactly matched the human EAAT2 sequence (Fig. 1). The sequence did not, however, match the human EAAT1, EAAT3, EAAT4, and EAAT5 sequences. This 62-kDa molecule was also immunoreactive to various anti-EAAT2 antibodies, including N19 (Santa Cruz Biotechnology), H85 (Santa Cruz Biotechnology), and the rabbit polyclonal anti-EAAT2 antibody HS5 (Fig. 1).

To examine the interaction between EAAT2 and p-tau, we conducted coimmunoprecipitation of homogenates from the frozen temporal cortex obtained from 4 AD, 2 PSP, 2 CBD, and 3 normal brains. We used HS5 for immunoprecipitation followed by immunoblotting with PHF1, a monoclonal antibody that recognizes pathological tau phosphorylated at residues Ser-396 and Ser-404, and a monoclonal tau antibody that recognizes all tau isoforms (Fig. 2A). Multiple tau bands of 30–60 kDa were recognized by the monoclonal tau antibody in all cases, whereas p-tau bands were detected only in crude extracts of AD, PSP, and CBD brains. As expected, only faint bands were recognized by PHF1 in normal brains. P-tau coprecipitated with the anti-EAAT2 antibody HS5 from AD, PSP, and CBD brains but not from normal brains. Larger amounts of tau coprecipitated with HS5 from AD, PSP, and CBD brains than those from normal brains (Fig. 2B). Coprecipitates of the anti-EAAT2 antibody were not stained with the tau1 antibody, which only recognized dephosphorylated tau (data not shown). Reverse coimmunoprecipitation experiments showed that larger amounts of EAAT2 coprecipitated with the monoclonal tau antibodies from AD, PSP, and CBD brains than those from normal brains. Thus, the tau protein that immunoprecipitated with the EAAT2 antibody was mainly p-tau. We performed immunoprecipitations in the absence or presence of an antibody for immunoprecipitations for determining antibody specificity for immunoprecipitation. We did not detect immunoreactivities in all immunoprecipitation experiments conducted in the absence of antibodies for immunoprecipitates (Fig. 2C).

To further determine the specificity of interaction between p-tau and EAAT2, we incubated nickel beads coupled either to recombinant His-tau, which was phosphorylated, or to a dephosphorylated control. Considerably larger amounts of EAAT2 were precipitated by p-tau than by dephosphorylated tau in all cases, suggesting that EAAT2 preferentially interacted with p-tau compared to dephosphorylated tau (Fig. 3A). The same amount of recombinant p-tau precipitated larger amounts of EAAT2 from AD, PSP, and CBD brains than from normal brains (Fig. 3B). These results suggest that p-tau more preferentially associates with EAAT2 in tauopathic brains than normal brains.

Interaction of EAAT2 with p-tau suggested that EAAT2 may localize in NFTs. In the midtemporal cortex, EAAT2 labeling occurred in large numbers of neuronal NFTs in all AD brains (Fig. 4A, B, and E), and in glial NFTs in PSP (Fig. 4C) and CBD brains (Fig. 4D). There was weak staining of glia and no obvious staining of neurons except for NFTs in AD, PSP, and CBD cases when the

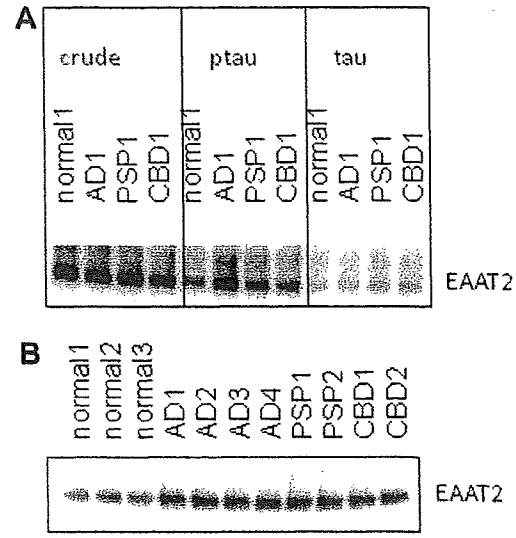

Fig. 3. Ability of EAAT2 to interact with phosphorylated tau (p-tau) was examined by a pull-down assay in which human brain homogenates were passed over 20 μL nickel beads coupled to His-phosphorylated tau or His-tau. Precipitated proteins were analyzed by the EAAT2 antibody.

samples were incubated with 70% formic acid. HS5 weakly stained ordinarily expressed glial EAAT2 but not NFTs when slides were incubated without 70% formic acid. Confocal microscopic examinations showed that EAAT2 was partially colocalized with p-tau, which was recognized by AT8 in NFTs of AD, PSP, and CBD brains (Fig. 4F–Q).

Immunoblots showed the expected serial extraction of tau with tau immunoreactivity in the sarkosyl-insoluble/formic acid-soluble fraction in AD patients but not in controls (Fig. 5A). Remarkably, EAAT2 and high-molecular-weight EAAT2 were also present in this fraction (Fig. 5A). EAAT2 was present in this fraction only in AD, PSP, and CBD brains (Fig. 5B).

4. Discussion

We have shown that EAAT2 interacts with p-tau in biochemical and histochemical studies. Immunoprecipitation studies indicated that EAAT2 preferentially associated with p-tau compared to dephosphorylated tau. A pull-down assay using recombinant tau or p-tau revealed that p-tau preferentially combined with EAAT2 from AD, PSP, or CBD brains compared to controls. Immunohistochemical studies showed that not only neuronal EAAT2 in AD brains but glial EAAT2 in PSP and CBD brains also colocalized with p-tau in NFTs. This suggests that EAAT2 may have been caught up with p-tau as tangles formed. Furthermore, we found high-molecular-weight EAAT2 in the sarkosyl-insoluble fraction. This suggests that EAAT2 may be oligomerized such as α-synuclein [15] and β-amyloid [16], which are major components of inclusions in neurodegenerative disorders.

EAATs are essential proteins for glutamate and aspartate uptake from the synaptic cleft into glias and neurons [17]. Several EAATs have been isolated and characterized [18]. EAAT1 is primarily localized in glia of the cerebellum and retina. EAAT2 is specifically located on astrocytes in non-diseased brains and is quantitatively dominant in the cortex [19]. EAAT2 is responsible for a majority of glutamate clearance in the adult forebrain [18]. A link among glutamate transporter dysfunction, increased extracellular glutamate levels, and the onset of excitotoxic neuronal damage has been established in AD and other neurodegenerative

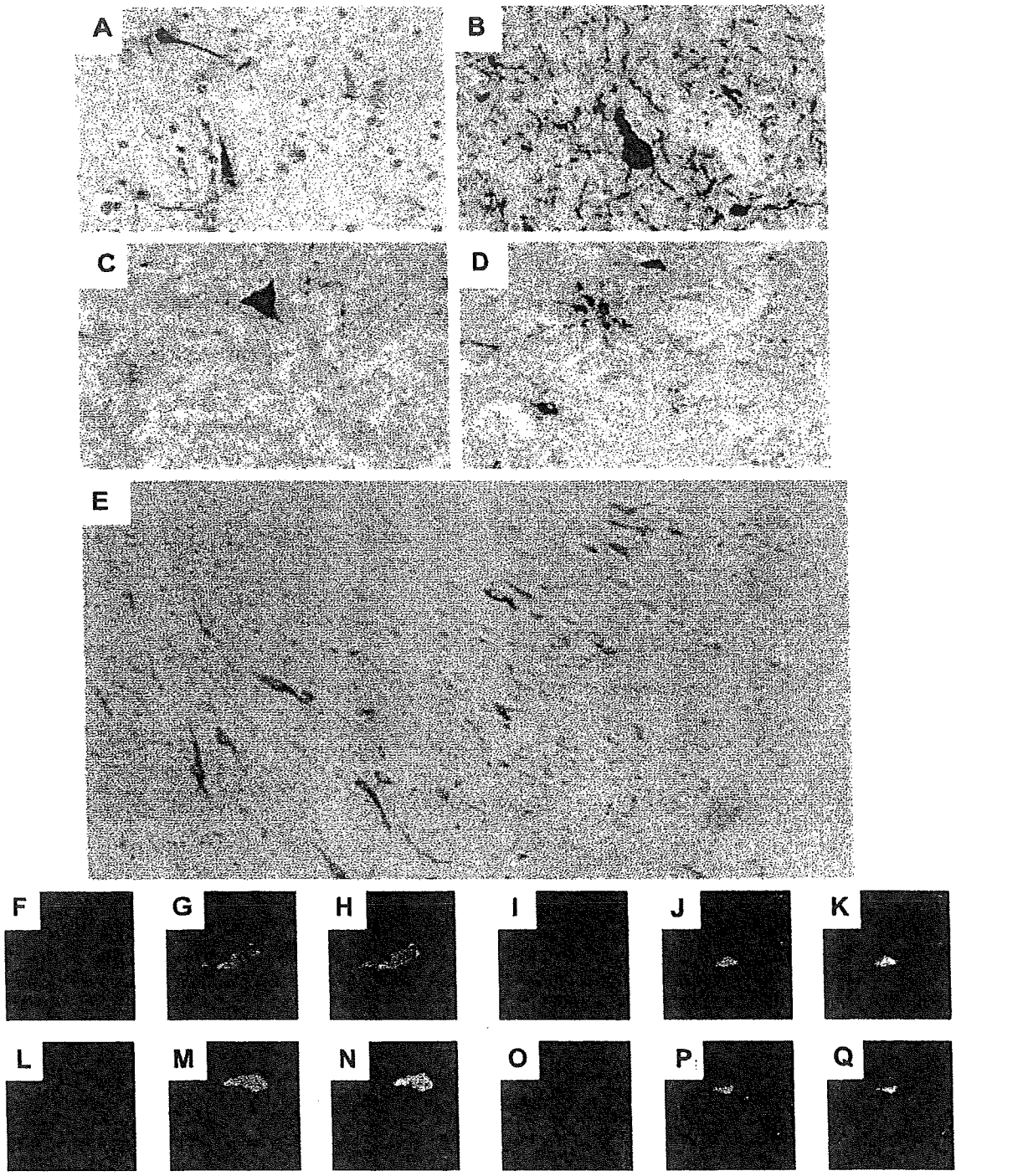

Fig. 4. Immunohistochemical analysis of EAAT2 in tauopathic specimens. (A–E) Neurofibrillary tangles (NFTs) in CA1 immunoreactive for EAAT2. Neuronal NFTs immunoreactive for EAAT2 in patients with AD (A, B, ×400) (E, ×100). Glial NFTs immunoreactive for EAAT2 in patients with PSP (C) or CBD (D, ×400). AD (F–K), PSP (L–N), and CBD (O–Q) double-labeling for EAAT2 (F, I, L and O) (green) or p-tau (G, J, M and P) (red). Merged images (H, K, N and Q) show the colocalization of p-tau and EAAT2. There is an overlap of the epitopes in some NFTs.

disorders [20]. Ablation of EAAT2 or glutamate transporter 1 (rodent homolog, GLT1) in mice has a significant effect on the development of pathogenic conditions and neurodegeneration [21]. The glial transport of excitatory amino acids in AD is deficient and the number of EAAT2-expressing cortical astrocytes is decreased [22].

In AD cases, expression of a glutamate transporter not normally found in neurons could imply that abnormal EAAT2 expression precedes and causes tangle formation in the affected neurons. Pull-down assays with recombinant p-tau showed that EAAT2 not only from AD but also from PSP and CBD brains preferentially interacted with p-tau. Thus, even physiologically expressed glial EAAT2 may be pathologically modified and subsequently bind with p-tau in pathological glia of PSP and CBD brains. This implies that neuronal and glial dysregulation of glutamate transport is strongly linked to the pathogenesis of tauopathies.

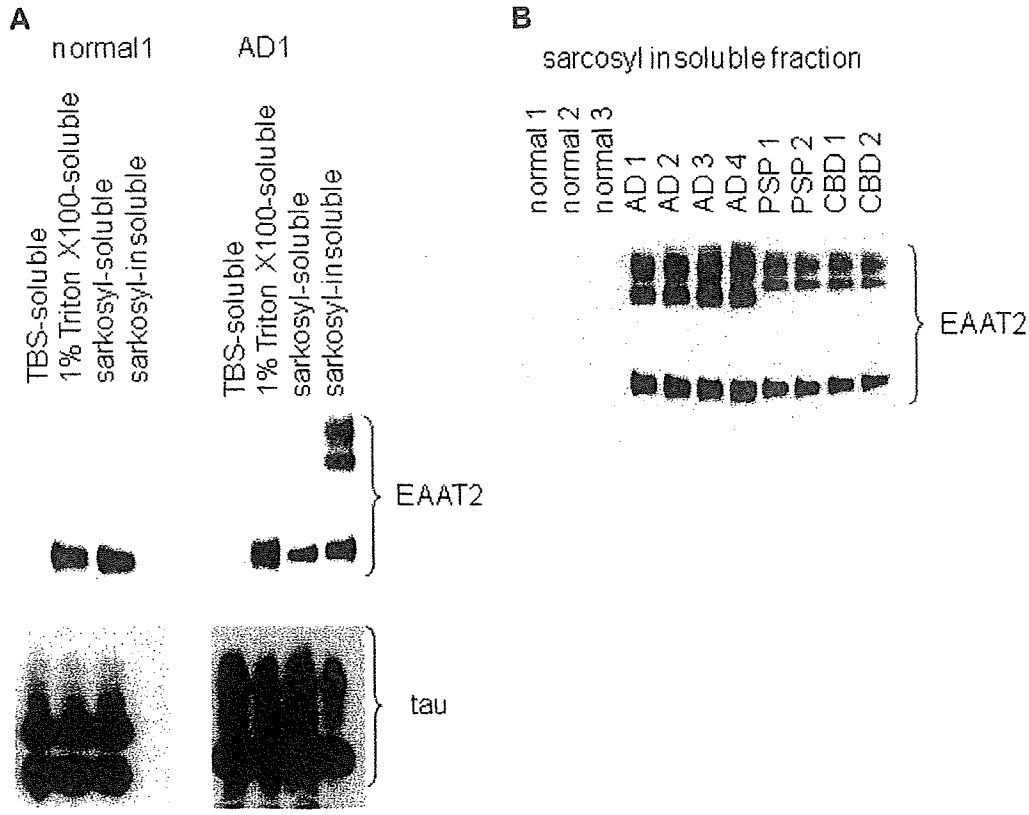

Fig. 5. Serial extractions of the temporal cortex were prepared from AD, PSP, CBD, and normal brains. (A) Preparation of supernatants and TBS-soluble, 1% Triton-X 100-soluble, sarkosyl-soluble, and sarkosyl-insoluble fractions are described in the Methods section. (B) Anti-EAAT2 immunoblots of sarkosyl-insoluble fraction from homogenates from AD, PSP, CBD, and normal brains.

Recently, it was shown that EAAT1 [23] and EAAT2 [24] were detected in NFT-bearing neurons but were not localized in NFTs of AD patients by immunohistochemical studies. Our results showed that EAAT2 is localized in NFTs. The difference between our results and those of previous studies is because of the different antibodies and immunohistochemical methods used. In our study, NFTs were not stained with our EAAT2 antibody due to the absence of using 70% formic acid to activate the antigens. Our EAAT2 antibody might be suitable for the detection of insoluble EAAT2 in immunohistochemical studies.

We therefore conclude that glutamate transport is altered in tauopathies with aberrant and physiological expression of EAAT2, and speculate that these changes occur before, but are related to, neurofibrillary pathology. These findings strongly implicate glutamate-mediated toxicity as an important mechanism in tauopathy-related neurodegeneration.

Acknowledgments

This study was supported by the Ministry of Education, Science, Sports, and Culture of Japan (H.S.).

References

[1] Buée, L., Bussière, T., Buée-Scherrer, V., Delacourte, A. and Hof, P.R. (2000) Tau protein isoforms, phosphorylation and role in neurodegenerative disorders. Brain Res. Rev. 33, 95–130.
[2] Hutton, M. (2000) Molecular genetics of chromosome 17 tauopathies. Ann. NY Acad. Sci. 920, 63–73.
[3] Trojanowski, J.Q. and Lee, V.M. (1995) Phosphorylation of paired helical filament tau in Alzheimer's disease neurofibrillary lesions: focusing on phosphatases. FASEB J. 9, 1570–1576.
[4] Kosik, K.S. (1990) Tau protein and neurodegeneration. Mol. Neurobiol. 4, 171–179.
[5] Geschwind, D.H. (2003) Tau phosphorylation, tangles, and neurodegeneration: the chicken or the egg? Neuron 40, 457–460.
[6] Noble, W. et al. (2003) Cdk5 is a key factor in tau aggregation and tangle formation in vivo. Neuron 38, 555–565.
[7] Jackson, G.R., Wiedau-Pazos, M., Sang, T.K., Wagle, N., Brown, C.A., Massachi, S. and Geschwind, D.H. (2002) Human wild-type tau interacts with wingless pathway components and produces neurofibrillary pathology in Drosophila. Neuron 34, 509–519.
[8] Shimura, H., Schwartz, D., Gygi, S.P. and Kosik, K.S. (2004) CHIP-Hsc70 complex ubiquitinates phosphorylated tau and enhances cell survival. J. Biol. Chem. 279, 4869–4876.
[9] Shimura, H., Miura-Shimura, Y. and Kosik, K.S. (2004) Binding of tau to heat shock protein 27 leads to decreased concentration of phosphorylated tau and enhanced cell survival. J. Biol. Chem. 279, 17957–17962.
[10] Rothstein, J.D., Jin, L., Dykes-Hoberg, M. and Kuncl, R.W. (1993) Chronic inhibition of glutamate uptake produces a model of slow neurotoxicity. Proc. Natl. Acad. Sci. USA 90, 6591–6595.
[11] Shimura, H., Schlossmacher, M.G., Hattori, N., Frosch, M.P., Trockenbacher, A., Schneider, R., Mizuno, Y., Kosik, K.S. and Selkoe, D.J. (2001) Ubiquitination of a new form of alpha-synuclein by parkin from human brain: implications for Parkinson's disease. Science 293, 263–269.
[12] Greenberg, S.G., Davies, P., Schein, J.D. and Binder, L.I. (1992) Hydrofluoric acid-treated tau PHF proteins display the same biochemical properties as normal tau. J. Biol. Chem. 267, 564–569.
[13] Shimura, H., Hattori, N., Kubo, S., Yoshikawa, M., Kitada, T., Matsumine, H., Asakawa, S., Minoshima, S., Yamamura, Y., Shimizu, N. and Mizuno, Y. (1999) Immunohistochemical and subcellular localization of Parkin protein: absence of protein in autosomal recessive juvenile parkinsonism patients. Ann. Neurol. 45, 668–672.
[14] Wang, Q., Woltjer, R.L., Cimino, P.J., Pan, C., Montine, K.S., Zhang, J. and Montine, T.J. (2005) Proteomic analysis of neurofibrillary tangles in Alzheimer disease identifies GAPDH as a detergent-insoluble paired helical filament tau binding protein. FASEB J. 19, 869–871.
[15] Goldberg, M.S. and Lansbury Jr., P.T. (2000) Is there a cause-and-effect relationship between alpha-synuclein fibrillization and Parkinson's disease? Nat. Cell Biol. 2, E115–E119.
[16] Walsh, D.M., Klyubin, I., Fadeeva, J.V., Cullen, W.K., Anwyl, R., Wolfe, M.S., Rowan, M.J. and Selkoe, D.J. (2002) Naturally secreted oligomers of amyloid

beta protein potently inhibit hippocampal long-term potentiation in vivo. Nature 416, 535–539.
[17] Scott, H.L., Tannenberg, A.E.G. and Dodd, P.R. (1995) Variant forms of neuronal glutamate transporter sites in Alzheimer disease cerebral cortex. J. Neurochem. 64, 2193–2202.
[18] Robinson, M.B. (1999) The family of sodium-dependent glutamate transporters: a focus on the GLT-1/EAAT2 subtype. Neurochem. Int. 33, 479–491.
[19] Arriza, J.L., Fairman, W.A., Wadiche, J.I., Murdoch, G.H., Kavanaugh, M.P. and Amara, S.G. (1994) Functional comparisons of three glutamate transporter subtypes cloned from human motor cortex. J. Neurosci. 14, 5559–5569.
[20] Dong, X.X., Wang, Y. and Qin, Z.H. (2009) Molecular mechanisms of excitotoxicity and their relevance to pathogenesis of neurodegenerative diseases. Acta Pharmacol. Sin. 30, 379–387.
[21] Tanaka, K. et al. (1997) Epilepsy and exacerbation of brain injury in mice lacking the glutamate transporter GLT-1. Science 276, 1699–1702.
[22] Masliah, E. et al. (1996) Deficient glutamate transport is associated with neurodegeneration in Alzheimer's disease. Ann. Neurol. 40, 759–766.
[23] Scott, H.L., Pow, D.V., Tannenberg, A.E. and Dodd, P.R. (2002) Aberrant expression of the glutamate transporter excitatory amino acid transporter 1 (EAAT1) in Alzheimer's disease. J. Neurosci. 22, RC206.
[24] Thai, D.R. (2002) Excitatory amino acid transporter EAAT-2 in tangle-bearing neurons in Alzheimer's disease. Brain Pathol. 12, 405–411.

nature genetics

LETTERS

Genome-wide association study identifies common variants at four loci as genetic risk factors for Parkinson's disease

Wataru Satake[1–3], Yuko Nakabayashi[1,2], Ikuko Mizuta[1,2], Yushi Hirota[1,2], Chiyomi Ito[1,2], Michiaki Kubo[4], Takahisa Kawaguchi[4], Tatsuhiko Tsunoda[4], Masahiko Watanabe[5], Atsushi Takeda[6], Hiroyuki Tomiyama[7], Kenji Nakashima[8], Kazuko Hasegawa[9], Fumiya Obata[10], Takeo Yoshikawa[11], Hideshi Kawakami[12], Saburo Sakoda[3], Mitsutoshi Yamamoto[13], Nobutaka Hattori[7], Miho Murata[14], Yusuke Nakamura[4,15] & Tatsushi Toda[1,2]

To identify susceptibility variants for Parkinson's disease (PD), we performed a genome-wide association study (GWAS) and two replication studies in a total of 2,011 cases and 18,381 controls from Japan. We identified a new susceptibility locus on 1q32 ($P = 1.52 \times 10^{-12}$) and designated this as *PARK16*, and we also identified *BST1* on 4p15 as a second new risk locus ($P = 3.94 \times 10^{-9}$). We also detected strong associations at *SNCA* on 4q22 ($P = 7.35 \times 10^{-17}$) and *LRRK2* on 12q12 ($P = 2.72 \times 10^{-8}$), both of which are implicated in autosomal dominant forms of parkinsonism. By comparing results of a GWAS performed on individuals of European ancestry, we identified *PARK16*, *SNCA* and *LRRK2* as shared risk loci for PD and *BST1* and *MAPT* as loci showing population differences. Our results identify two new PD susceptibility loci, show involvement of autosomal dominant parkinsonism loci in typical PD and suggest that population differences contribute to genetic heterogeneity in PD.

Parkinson's disease (MIM168600) is one of the most common neurodegenerative diseases worldwide, affecting 1–2% of individuals aged ≥65 years[1]. Clinical features of PD result primarily from loss of dopaminergic neurons in the substantia nigra. Various medical treatments improve PD symptoms but do little to deter disease progression. Identifying genetic risk factors for PD will be helpful in elucidating the pathogenesis of the disease. Linkage studies have been successful in mapping genes for mendelian forms of parkinsonism: *SNCA* (encoding α-synuclein)[2] and *LRRK2* (refs. 3,4) in autosomal dominant forms, and *PARK2* (encoding parkin), *PINK1*, *PARK7* (encoding DJ-1) and *ATP13A2* in autosomal recessive forms[5,6]. However, mendelian forms of parkinsonism are rare compared to the far more common typical PD, a complex disorder caused by multiple genetic and environmental factors[7]. Association studies have evaluated variants in many candidate genes for PD[7], but only a few, such as common variants of *SNCA*[8–10] and rare mutations of *GBA*[11], have been identified as PD-susceptibility genes with genome-wide significance. Recently, GWASs in PD have provided association evidence at several loci, but not at the genome-wide significant level[12–14].

We conducted a GWAS and two subsequent replication studies for PD to identify further common variants that contribute to disease. In the GWAS stage, we genotyped 561,288 SNPs on autosomal and sex chromosomes using the HumanHap550 array (Illumina). The GWAS stage included 1,078 PD cases and 2,628 controls in the Japanese population (**Supplementary Note**). After SNP and sample quality control analyses, we used genotype data from 435,470 SNPs in 988 cases and 2,521 controls in the GWAS analysis (see Online Methods).

We tested for association between each SNP and PD using the Cochran-Armitage trend test with 1 d.f. The quantile-quantile plot showed a close match to test statistics expected under the null distribution (genomic inflation factor $\lambda = 1.055$ for PD) (**Fig. 1a,b**). This indicates minimal overall inflation of genome-wide statistical results due to population stratification and also reveals a number of SNPs whose *P* values exceed those expected under the null hypothesis. Seventeen SNPs showed $P < 5 \times 10^{-7}$, the threshold for genome-wide significance suggested by the Wellcome Trust Case Control Consortium[15] (**Fig. 1c**). All these SNPs were located on 4q22, a region harboring *SNCA* that was previously identified by us and others as a definite susceptibility gene for PD[8–10].

[1]Division of Neurology/Molecular Brain Science, Kobe University Graduate School of Medicine, Kobe, Japan. [2]Division of Clinical Genetics, Osaka University Graduate School of Medicine, Suita, Japan. [3]Department of Neurology, Osaka University Graduate School of Medicine, Suita, Japan. [4]Center for Genomic Medicine, RIKEN, Yokohama, Japan. [5]Department of Neurology, Graduate School of Comprehensive Human Sciences, University of Tsukuba, Tsukuba, Japan. [6]Division of Neurology, Tohoku University Graduate School of Medicine, Sendai, Japan. [7]Department of Neurology, Juntendo University School of Medicine, Tokyo, Japan. [8]Department of Neurology, Tottori University Faculty of Medicine, Yonago, Japan. [9]Department of Neurology, Sagamihara National Hospital, Sagamihara, Japan. [10]Division of Clinical Immunology, Graduate School of Medical Sciences, Kitasato University, Sagamihara, Japan. [11]RIKEN Brain Science Institute, Saitama, Japan. [12]Department of Epidemiology, Research Institute for Radiation Biology and Medicine, Hiroshima University, Hiroshima, Japan. [13]Department of Neurology, Kagawa Prefectural Central Hospital, Takamatsu, Japan. [14]Department of Neurology, National Center Hospital of Neurology and Psychiatry, Kodaira, Japan. [15]Human Genome Center, Institute of Medical Science, University of Tokyo, Tokyo, Japan. Correspondence should be addressed to T.Toda (toda@med.kobe-u.ac.jp).

Received 5 June; accepted 21 October; published online 15 November 2009; doi:10.1038/ng.485

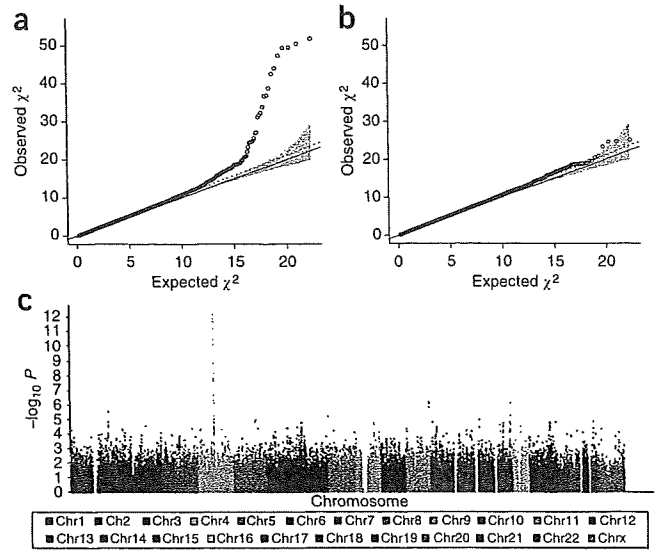

Figure 1 Genome-wide association results from the discovery phase. (**a**) Quantile-quantile plot for test statistics (Cochran-Armitage trend test) for 435,470 SNPs passing quality control. The solid line represents concordance of observed and expected values. Slope of the dashed line represents the genomic inflation factor ($\lambda = 1.055$). The shaded region is the 95% concentration band formed by calculating, for each order statistic, the 2.5th and 97.5th percentiles of the respective distribution under the null hypothesis. (**b**) Quantile-quantile plot for test statistics (Cochran-Armitage trend test) after the removal of the four loci with strong associations in this study (1q32, 4p15, 4q22 and 12q12). (**c**) Manhattan plot presenting the *P* values across the genome. The $-\log_{10} P$ (Cochran-Armitage trend test) from 435,470 SNPs in 988 Parkinson's disease cases and 2,521 controls is plotted according to its physical position on successive chromosomes.

For fast-track replication, we selected the 337 most associated SNPs ($P \leq 0.000533$) from analysis of GWAS data and genotyped them in a sample set of replication 1, which consisted of 612 cases and 14,139 controls from Japan (**Supplementary Note**). Thirty-two SNPs showed association of $P < 0.05$ in replication 1 (**Supplementary Fig. 1**). Combined analyses of the GWAS and replication 1 showed that 12 SNPs in 3 loci (1q32, 4p15 and 4q22) surpassed $P < 5 \times 10^{-7}$. Furthermore, we found association signals ($P = 3.06 \times 10^{-6}$, OR = 1.36) on 12q12, harboring *LRRK2*, which is a causative gene for autosomal dominant parkinsonism (**Table 1**).

In replication 2, we tested 24 SNPs at these four loci for association with PD. An independent sample set (321 cases and 1,614 controls) recruited from Japan was used in replication 2 (**Supplementary Note**). Association evidence was again found at these four loci: 1q32, $P = 2.80 \times 10^{-4}$, OR = 1.37; 4p15, $P = 7.70 \times 10^{-3}$, OR = 1.26; 4q22, $P = 0.02$, OR = 1.22; and 12q12, $P = 6.43 \times 10^{-4}$, OR = 1.57 (**Table 1**). The disease associations on 1q32 and 12q12 exceeded the conservative Bonferroni-corrected threshold for significance ($P = 0.0021$; calculated as 0.05/24). All the SNPs showed allele frequency differences in the same direction in the GWAS, replication 1 and replication 2. Furthermore, combined analysis of the GWAS and two replication stages provided strong evidence of association in the four regions with a significance level of $P = 2.72 \times 10^{-8}$ or less (**Table 1**).

We identified two new susceptibility loci with genome-wide significance on 1q32 and 4p15, which have not been reported to be associated with PD in previous studies[12–14]. On 1q32, seven SNPs (rs16856139, rs823128, rs823122, rs947211, rs823156, rs708730 and rs11240572) reached $P < 5 \times 10^{-7}$ in the overall analysis (**Fig. 2a**). rs947211 showed the strongest association to PD ($P = 1.52 \times 10^{-12}$, OR = 1.30) and is located 8.5 kb upstream of *RAB7L1* and 5.6 kb downstream of *SLC41A1*. Linkage disequilibrium (LD) analysis revealed that SNPs with significant associations to PD lie within several LD blocks containing the following five genes: *SLC45A3*, *NUCKS1*, *RAB7L1*, *SLC41A1* and *PM20D1* (also called *FLJ32569*) (**Table 1** and **Fig. 2a**). Three genes (*NUCKS1*, *RAB7L1* and *SLC41A1*) were contained in the same LD block as rs947211. rs947211 was weakly correlated with the other six SNPs ($r^2 = 0.07$–0.25), and we observed residual association signals when rs947211 and each of the other six SNPs were paired in conditional analyses of our overall data. This result suggests that this locus has multiple independent association signals (**Supplementary Table 1**). These data provide the first evidence, to our knowledge, of an association between 1q32 and PD susceptibility, and we designated this region as *PARK16*.

On 4p15, four SNPs (rs11931532, rs12645693, rs4698412 and rs4538475) reached $P < 5 \times 10^{-7}$ in the combined analysis (**Fig. 2b**). These four SNPs showed strong disease association with almost the same significance levels (ranging from $P = 3.94 \times 10^{-9}$ to $P = 1.78 \times 10^{-8}$, all OR = 1.24); among them, rs4538475 was the most strongly associated. The four SNPs were located from intron 8 to 4.1 kb downstream of *BST1* (bone marrow stromal cell antigen). LD analysis revealed that the four SNPs were correlated with $r^2 > 0.78$ and lie within a 15 kb LD block containing a single gene, *BST1*.

The remaining two intervals (4q22 and 12q12) harbored genes previously found to be causal for autosomal dominant forms of parkinsonism, specifically, *SNCA* and *LRRK2*, respectively. On 4q22, seven SNPs (rs3733449, rs11931074, rs3857059, rs2736990, rs3796661, rs6532194 and rs12233759) throughout the *SNCA* region showed genome-wide significant association in the combined analysis (**Fig. 2c**). The most significantly associated SNPs, rs11931074 ($P = 7.35 \times 10^{-17}$, OR = 1.37) and rs3857059 ($P = 5.68 \times 10^{-16}$, OR = 1.36), are approximately 35.7 kb apart, located 7.2 kb downstream from and in intron 4 of *SNCA*, respectively. The entire *SNCA* gene was divided into two LD blocks at intron 4. Both SNPs were positioned on the 3′ side of the LD block and showed a high degree of LD ($r^2 = 0.98$). Three SNPs (rs2736990, rs3796661 and rs6532194) were moderately correlated with rs11931074 ($r^2 = 0.81$, 0.76 and 0.63, respectively). The remaining two SNPs (rs3733449 and rs12233759) were weakly correlated with rs11931074 ($r^2 = 0.05$ and 0.24, respectively), and residual association signals were marginally observed when rs11931074 and each of these two SNPs were paired in conditional analyses of our overall data (**Supplementary Table 1**). These data confirm *SNCA* as a susceptibility gene for PD.

On 12q12, five SNPs (rs1994090, rs7304279, rs4768212, rs2708453 and rs2046932) surpassed $P < 5 \times 10^{-7}$ in the overall analysis (**Fig. 2d**). The five SNPs showed strong disease association with almost the same significance (ranging from $P = 2.72 \times 10^{-8}$ to $P = 1.09 \times 10^{-7}$, OR = 1.37–1.39); among them, rs1994090 was the most strongly associated to PD. These five SNPs were located from intron 2 of *SLC2A13* to 38.4 kb upstream of *LRRK2*. These SNPs were highly correlated with $r^2 > 0.83$ and were positioned within several LD blocks defined by the method of Gabriel *et al.*[16]. This is the first evidence that common variants proximal to *LRRK2* are associated with PD at genome-wide significance level.

Variants with the highest significance at the four loci detected in this study were common SNPs with risk allele frequencies of 0.50 (rs947211 on 1q32), 0.38 (rs4538475 on 4p15), 0.58 (rs11931074 on 4q22) and 0.08 (rs1994090 on 12q12) (**Table 1**). Population attributable risks for rs947211, rs4538475, rs11931074 and rs1994090 were estimated to be 13%, 8%, 18% and 3%, respectively.

Table 1 Summary of association results for representative SNPs that characterize the association of Parkinson's disease with 1q32 (*PARK16*), 4p15 (*BST1*), 4q22 (*SNCA*) and 12q12 (*LRRK2*)

				GWAS			Replication 1			GWAS + Replication 1		Replication 2			GWAS + Replication 1+2	
			Allele	MAF			MAF					MAF				
Locus	SNP	Pos (Mb)	Minor/ major	Case Ctrl	P_{trend}	OR (95% CI)	Case Ctrl	P_{trend}	OR (95% CI)	P_{cmh}	OR (95% CI)	Case Ctrl	P_{trend}	OR (95% CI)	P_{cmh}	OR (95% CI)
New PD loci																
1q32	rs16856139	203.91	T/C	0.10	2.55×10^{-6}	1.50	0.11	0.067	1.19	2.15×10^{-6}	1.35	0.10	0.015	1.42	1.02×10^{-7}	1.36
(*PARK16*)				0.14		(1.26–1.77)	0.13		(0.99–1.44)		(1.19–1.54)	0.13		(1.07–1.88)		(1.22–1.53)
	rs823128	203.98	G/A	0.10	2.09×10^{-5}	1.43	0.11	0.0056	1.31	4.67×10^{-7}	1.38	0.09	0.0028	1.53	4.88×10^{-9}	1.41
				0.14		(1.21–1.69)	0.13		(1.08–1.59)		(1.22–1.57)	0.14		(1.16–2.03)		(1.26–1.58)
	rs823122	203.99	C/T	0.10	7.98×10^{-5}	1.39	0.11	0.013	1.27	3.87×10^{-6}	1.34	0.09	0.0034	1.52	5.22×10^{-8}	1.37
				0.14		(1.18–1.64)	0.13		(1.05–1.54)		(1.18–1.52)	0.14		(1.15–2.01)		(1.22–1.54)
	rs947211	204.02	A/G	0.43	1.15×10^{-4}	1.23	0.42	1.35×10^{-6}	1.35	1.12×10^{-9}	1.28	0.42	2.80×10^{-4}	1.37	1.52×10^{-12}	1.30
				0.48		(1.11–1.37)	0.50		(1.19–1.52)		(1.18–1.38)	0.50		(1.16–1.63)		(1.21–1.39)
	rs823156	204.03	G/A	0.13	1.20×10^{-5}	1.40	0.14	0.012	1.25	6.45×10^{-7}	1.33	0.12	0.0013	1.52	3.60×10^{-9}	1.37
				0.17		(1.20–1.62)	0.17		(1.05–1.48)		(1.19–1.49)	0.17		(1.17–1.95)		(1.23–1.52)
	rs708730	204.04	G/A	0.14	2.60×10^{-5}	1.37	0.15	0.022	1.22	2.89×10^{-6}	1.30	0.12	0.0019	1.48	2.43×10^{-8}	1.33
				0.18		(1.18–1.59)	0.17		(1.03–1.44)		(1.17–1.46)	0.18		(1.15–1.89)		(1.21–1.48)
	rs11240572	204.07	A/C	0.13	1.66×10^{-4}	1.34	0.13	0.016	1.24	9.78×10^{-6}	1.30	0.12	0.0024	1.49	1.08×10^{-7}	1.33
				0.16		(1.15–1.56)	0.16		(1.04–1.48)		(1.16–1.46)	0.17		(1.15–1.92)		(1.20–1.48)
4p15	rs11931532	15.33	T/C	0.45	2.75×10^{-4}	1.22	0.47	1.86×10^{-4}	1.26	2.02×10^{-7}	1.23	0.47	0.0077	1.26	5.13×10^{-9}	1.24
(*BST1*)				0.40		(1.09–1.35)	0.42		(1.11–1.42)		(1.14–1.34)	0.41		(1.06–1.49)		(1.15–1.33)
	rs12645693	15.34	G/A	0.45	3.06×10^{-4}	1.21	0.47	3.00×10^{-4}	1.25	3.42×10^{-7}	1.23	0.47	0.0077	1.26	8.65×10^{-9}	1.24
				0.40		(1.09–1.35)	0.42		(1.11–1.41)		(1.14–1.33)	0.41		(1.06–1.49)		(1.15–1.33)
	rs4698412	15.35	A/G	0.38	5.28×10^{-5}	1.25	0.40	4.91×10^{-4}	1.24	1.03×10^{-7}	1.25	0.38	0.055	1.19	1.78×10^{-8}	1.24
				0.33		(1.12–1.40)	0.35		(1.10–1.40)		(1.15–1.35)	0.34		(1.00–1.42)		(1.15–1.33)
	rs4538475	15.35	A/G	0.41	4.05×10^{-5}	1.25	0.43	3.48×10^{-4}	1.25	5.98×10^{-8}	1.25	0.42	0.022	1.22	3.94×10^{-9}	1.24
				0.36		(1.12–1.40)	0.38		(1.10–1.41)		(1.15–1.35)	0.37		(1.03–1.46)		(1.16–1.34)
Loci located in or near autosomal dominant parkinsonism genes																
4q22	rs11931074	90.86	G/T	0.32	6.17×10^{-13}	1.50	0.36	2.12×10^{-5}	1.31	2.19×10^{-16}	1.41	0.38	0.034	1.21	7.35×10^{-17}	1.37
(*SNCA*)				0.42		(1.34–1.68)	0.42		(1.16–1.48)		(1.30–1.53)	0.43		(1.01–1.44)		(1.27–1.48)
	rs3857059	90.89	A/G	0.32	1.17×10^{-12}	1.49	0.36	6.92×10^{-5}	1.29	1.54×10^{-15}	1.40	0.38	0.041	1.20	5.68×10^{-16}	1.36
				0.41		(1.34–1.67)	0.42		(1.14–1.45)		(1.29–1.52)	0.43		(1.01–1.43)		(1.26–1.46)
	rs894278	90.95	G/T	0.43	7.68×10^{-5}	1.24	0.39	0.46	1.05	4.77×10^{-4}	1.15	0.42	0.020	1.22	3.28×10^{-5}	1.17
				0.38		(1.11–1.37)	0.38		(0.93–1.18)		(1.07–1.25)	0.37		(1.03–1.45)		(1.09–1.25)
	rs6532194	91.00	C/T	0.31	6.93×10^{-11}	1.44	0.36	0.0014	1.22	1.77×10^{-12}	1.35	0.37	0.040	1.21	4.15×10^{-13}	1.32
				0.40		(1.29–1.61)	0.41		(1.08–1.39)		(1.24–1.46)	0.41		(1.01–1.44)		(1.22–1.42)
12q12	rs1994090	38.71	G/T	0.11	4.45×10^{-5}	1.43	0.10	0.018	1.26	3.06×10^{-6}	1.36	0.12	0.0019	1.51	2.72×10^{-8}	1.39
(*LRRK2*)				0.08		(1.20–1.70)	0.08		(1.04–1.54)		(1.20–1.55)	0.08		(1.16–1.97)		(1.24–1.56)
	rs7304279	38.75	T/C	0.11	5.17×10^{-5}	1.42	0.10	0.026	1.25	5.10×10^{-6}	1.35	0.12	0.0022	1.50	5.06×10^{-8}	1.38
				0.08		(1.20–1.69)	0.08		(1.03–1.52)		(1.19–1.54)	0.09		(1.15–1.95)		(1.23–1.55)
	rs4768212	38.76	C/T	0.11	3.98×10^{-5}	1.43	0.10	0.057	1.21	1.10×10^{-5}	1.34	0.12	0.0020	1.51	1.09×10^{-7}	1.37
				0.08		(1.20–1.70)	0.08		(0.99–1.48)		(1.18–1.52)	0.08		(1.16–1.97)		(1.22–1.54)
	rs2708453	38.76	T/G	0.11	7.46×10^{-5}	1.41	0.10	0.063	1.21	2.04×10^{-5}	1.33	0.13	6.43×10^{-4}	1.57	9.67×10^{-8}	1.38
				0.08		(1.19–1.68)	0.08		(0.99–1.48)		(1.17–1.52)	0.08		(1.21–2.04)		(1.22–1.55)
	rs2046932	38.87	T/C	0.11	3.24×10^{-5}	1.44	0.10	0.039	1.23	5.47×10^{-6}	1.35	0.13	0.0017	1.52	4.34×10^{-8}	1.39
				0.08		(1.21–1.71)	0.08		(1.01–1.51)		(1.19–1.54)	0.09		(1.17–1.97)		(1.23–1.56)

Nucleotide positions refer to NCBI build 36. *P* values obtained in the case-control analysis using the Cochran-Armitage trend test (1 d.f.) are listed (P_{trend}). Combined *P* values (P_{cmh}) and combined ORs of the Cochran-Mantel-Haenzel test statistics are shown. MAF, minor allele frequency.

Next, we exchanged data with colleagues performing a GWAS of PD in individuals of European ancestry[17]. Their study found a strong association at the *MAPT* (microtubule-associated protein tau) region on 17q21. We genotyped our samples for six SNPs at the *MAPT* locus to evaluate these associations in the Asian population; however, the association with *MAPT* was not replicated in our study (**Supplementary Table 2** and **Supplementary Fig. 2**). Conversely, despite strong association signals in our scan of the samples from the Asian population, the association with *BST1* on 4p15 was not detected among individuals of European ancestry[17]. In contrast, the associations we found with *PARK16* and *LRRK2* were replicated among individuals of European ancestry[17]. These data provide evidence that *PARK16* and *LRRK2*, in addition to *SNCA*, are PD risk loci common to Asian- and European-descent populations and indicate that there is population genetic heterogeneity in the *MAPT* region and 4p15 (*BST1*) for PD susceptibility.

The *PARK16* region contains functionally interesting candidate genes for PD etiology. SLC41A1 is a magnesium (Mg^{2+}) transporter[18]. It is of interest that Mg^{2+} deficiency is thought to be an environmental risk factor for the amyotrophic lateral sclerosis

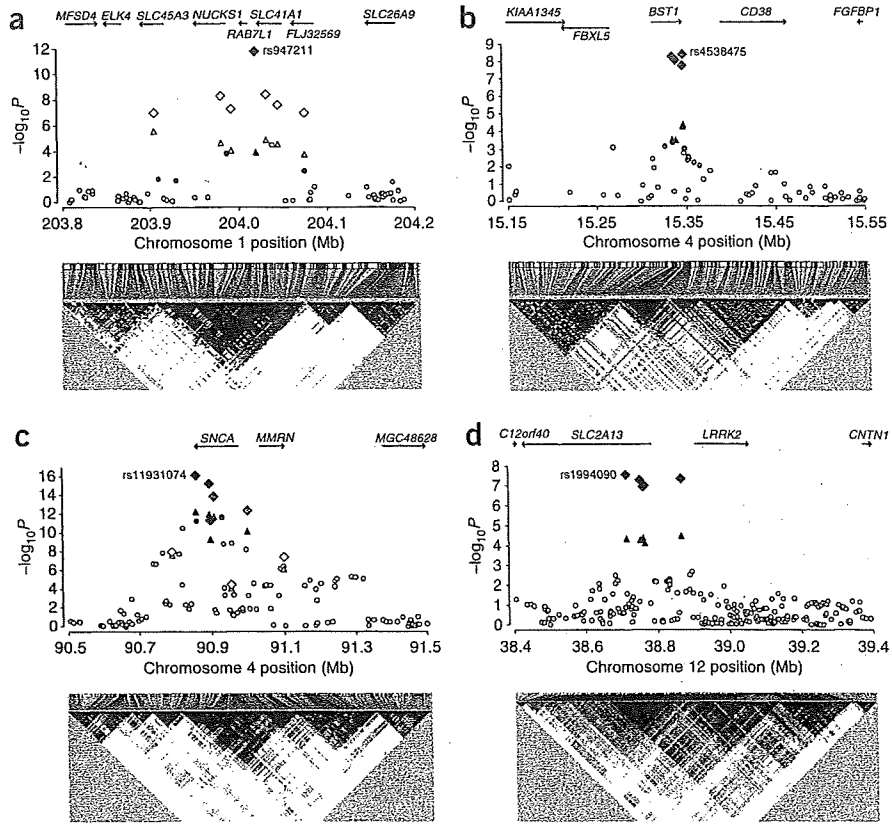

Figure 2 Regional association plots and linkage disequilibrium structure for the four PD risk loci. (**a**) 1q32 (*PARK16*). (**b**) 4p15 (*BST1*). (**c**) 4q22 (*SNCA*). (**d**) 12q12 (*LRRK2*). The $-\log_{10}$ *P* (Cochran-Armitage trend test) for association in the GWAS stage of SNPs across each region are shown as small triangles for SNPs that were selected for replication and as small circles for SNPs not selected. The $-\log_{10}$ combined *P* values (Cochran-Mantel-Haenszel test) for association in overall samples of SNPs selected for replication are shown as large diamonds. In each panel, the SNP with the most significant association in the combined analysis is listed. Proxies are indicated with colors determined from their pairwise r^2 from the JPT and CHB HapMap data (red, $r^2 > 0.8$; orange, $r^2 = 0.5$–0.8; yellow, $r^2 = 0.2$–0.5; white, $r^2 < 0.2$ or no information available). Positions are NCBI build 36 coordinates.

(ALS)-parkinsonism/dementia complex (MIM105500)[19]. Furthermore, RAB7L1 is a small GTP-binding protein that plays an important role in regulation of exo- and endocytotic pathways[20], and NUCKS1 is a nuclear protein containing several consensus phosphorylation sites for casein kinase II and cyclin-dependent kinases of unknown function[21]. We evaluated the relationships between the PD-associated SNPs and the transcript levels of genes in an available genome-wide gene expression database[22]. We found that rs947211 and ten tightly linked HapMap SNPs ($r^2 > 0.9$) were strongly associated with transcript levels of *NUCKS1* (rs947211, $P = 6.0 \times 10^{-15}$; rs823114, $P = 2.7 \times 10^{-34}$). These PD-susceptibility variants are the principal genetic determinants of variation in expression levels of *NUCKS1* (**Supplementary Fig. 3**). These data highlight *NUCKS1* as a promising candidate for association with PD that is worthy of additional follow-up.

The product of *BST1* on 4p15 catalyses formation of cyclic ADP-ribose (cADPR)[23]. cADPR mobilizes calcium (Ca^{2+}) from ryanodine-sensitive intracellular Ca^{2+} stores in the endoplasmic reticulum[24]. Disruption of Ca^{2+} homeostasis has recently been proposed as a possible cause of selective vulnerability of dopaminergic neurons in PD[25–27]. Associated SNPs in the *BST1* region may modify ADP-ribosylcyclase activity, thus leading to Ca^{2+} dyshomeostasis in dopaminergic neurons.

Two of the four susceptibility loci detected in our scan contained genes linked to autosomal dominant forms of parkinsonism. Gene overdosage is a potential mechanism for the influence of *SNCA* on PD because triplication and duplication of the *SNCA* locus has been seen in families with autosomal dominant parkinsonism[28]. SNPs with prominently low *P* values compared to other SNPs in the region were around the 3′ region of *SNCA*; these SNPs may function as enhancer or silencer elements, improve RNA stability or influence alternative splicing. The associated interval on 12q12 contains *SLC2A13* and the region upstream of *LRRK2*. Given prior evidence, *LRRK2* stands out as the most likely susceptibility gene for PD, although it remains possible that *SLC2A13*, which encodes a H^+-myoinositol cotransporter, may be the PD-related gene in this region[29]. Previous reports have investigated the association of SNPs in *LRRK2* with PD, but the results are a subject of dispute[30,31]. In the present study, it is noteworthy that the PD-associated intervals lie upstream of *LRRK2*. Increased kinase activity of mutant LRRK2 mediates neuronal toxicity[32,33]. PD-associated SNPs may play a role in transcriptional upregulation of *LRRK2*, leading to loss of dopaminergic neurons.

SNCA is a main component of Lewy bodies, a pathological hallmark of typical PD. The clinical features of individuals with *SNCA* duplication or *LRRK2* mutation similar to typical PD. 1.6% of sporadic PD cases among individuals of European ancestry have heterozygous *LRRK2* G2019S mutations[34]. These data support the close involvement of these genes with sporadic PD. Our data clearly show that the genes involved in autosomal dominant parkinsonism play a large part in the complex etiology of typical PD. Genes that cause autosomal dominant parkinsonism through their causative mutations also confer risk of typical PD through their common variants. Although further research is needed, this relationship between rare single-gene disorders and common multifactorial disorders may also be applicable for other disorders beyond PD.

Finally, *MAPT* mutations cause hereditary frontotemporal dementia and parkinsonism linked to chromosome 17 (FTDP-17), a type of autosomal dominant parkinsonism[35], and the *MAPT* H1 haplotype has been reported to be associated with several tauopathies[36–38]. Although the *MAPT* region is divided into two major haplotypes, H1 and H2, in Europeans, the H2 haplotype is absent in East Asians. Therefore, we believe that the differences observed between our study and the findings in populations of European descent reflect population differences in the genetic heterogeneity of PD etiology, although differences in allele frequencies and LD structure and a possible difference in the effect size between the European and East Asian populations may influence the detection power of the two scans.

Further increases in sample sizes for SNP-GWAS efforts and searches for copy number variation and rare variants will reveal additional genetic risk factors and further enhance our understanding of PD.

METHODS

Methods and any associated references are available in the online version of the paper at http://www.nature.com/naturegenetics/.

Note: Supplementary information is available on the Nature Genetics website.

ACKNOWLEDGMENTS

We are grateful to the individuals with PD who participated in this study. We also thank T. Takeshima and E. Ohta for PD samples, H. Inoko and K. Tokunaga for control samples, M. Kanagawa and K. Ura for editing, K. Yasuno and R. Ashida for analyses, and K. Yamada for genotyping. We appreciate all the volunteers and participating institutions of BioBank Japan for samples. This work was supported by a grant from Core Research for Evolutional Science and Technology (CREST), Japan Science and Technology Agency (JST); by the Global COE program and KAKENHI (17019044 and 19590990), both from the Ministry of Education, Culture, Sports, Science and Technology of Japan; and by the Grant-in-Aid for 'the Research Committee for the Neurodegenerative Diseases' of the Research on Measures for Intractable Diseases and Research Grant (H19-Genome-Ippan-001), all from the Ministry of Health, Labor and Welfare of Japan.

AUTHOR CONTRIBUTIONS

T. Toda conceived the study. W.S., I.M. and T. Toda designed the study. W.S., Y.N., C.I., M.K. and T.Y. performed genotyping. W.S. and T. Toda wrote the manuscript. W.S., T.K. and T. Tsunoda performed data analysis. W.S., I.M., Y.H., M.W., A.T., H.T., K.N., K.H., F.O., H.K., S.S., M.Y., N.H., M.M. and T. Toda managed Parkinson clinical information and DNA samples. M.K. and Y.N. managed DNA samples belonging to BioBank Japan. T. Toda obtained funding for the study.

Published online at http://www.nature.com/naturegenetics/.
Reprints and permissions information is available online at http://npg.nature.com/reprintsandpermissions/.

1. de Rijk, M.C. *et al.* Prevalence of parkinsonism and Parkinson's disease in Europe: the EUROPARKINSON collaborative study. *J. Neurol. Neurosurg. Psychiatry* **62**, 10–15 (1997).
2. Polymeropoulos, M.H. *et al.* Mutation in the α-synuclein gene identified in families with Parkinson's disease. *Science* **276**, 2045–2047 (1997).
3. Paisán-Ruíz, C. *et al.* Cloning of the gene containing mutations that cause *PARK8*-linked Parkinson's disease. *Neuron* **44**, 595–600 (2004).
4. Zimprich, A. *et al.* Mutations in *LRRK2* cause autosomal-dominant parkinsonism with pleomorphic pathology. *Neuron* **44**, 601–607 (2004).
5. Farrer, M.J. Genetics of Parkinson disease: paradigm shifts and future prospects. *Nat. Rev. Genet.* **7**, 306–318 (2006).
6. Thomas, B. & Beal, M.F. Parkinson's disease. *Hum. Mol. Genet.* **16 Spec No. 2**, R183–R194 (2007).
7. Warner, T.T. & Schapira, A.H. Genetic and environmental factors in the cause of Parkinson's disease. *Ann. Neurol.* **53**(Suppl 3), S16–S23 (2003).
8. Pals, P. *et al.* α-Synuclein promoter confers susceptibility to Parkinson's disease. *Ann. Neurol.* **56**, 591–595 (2004).
9. Mizuta, I. *et al.* Multiple candidate gene analysis identifies α-synuclein as a susceptibility gene for sporadic Parkinson's disease. *Hum. Mol. Genet.* **15**, 1151–1158 (2006).
10. Müller, J.C. *et al.* Multiple regions of α-synuclein are associated with Parkinson's disease. *Ann. Neurol.* **57**, 535–541 (2005).
11. Aharon-Peretz, J., Rosenbaum, H. & Gershoni-Baruch, R. Mutations in the glucocerebrosidase gene and Parkinson's disease in Ashkenazi Jews. *N. Engl. J. Med.* **351**, 1972–1977 (2004).
12. Maraganore, D.M. *et al.* High-resolution whole-genome association study of Parkinson disease. *Am. J. Hum. Genet.* **77**, 685–693 (2005).
13. Fung, H.C. *et al.* Genome-wide genotyping in Parkinson's disease and neurologically normal controls: first stage analysis and public release of data. *Lancet Neurol.* **5**, 911–916 (2006).
14. Pankratz, N. *et al.* Genomewide association study for susceptibility genes contributing to familial Parkinson disease. *Hum. Genet.* **124**, 593–605 (2009).
15. Welcome Trust Case Control Consortium. Genome-wide association study of 14,000 cases of seven common diseases and 3,000 shared controls. *Nature* **447**, 661–678 (2007).
16. Gabriel, S.B. *et al.* The structure of haplotype blocks in the human genome. *Science* **296**, 2225–2229 (2002).
17. Simón-Sánchez, J. *et al.* Genome-wide association study reveals genetic risk underlying Parkinson's disease. *Nat. Genet.* advance online publication, doi:10.1038/ng.487 (15 November 2009).
18. Kolisek, M. *et al.* SLC41A1 is a novel mammalian Mg^{2+} carrier. *J. Biol. Chem.* **283**, 16235–16247 (2008).
19. Garruto, R.M. *et al.* Disappearance of high-incidence amyotrophic lateral sclerosis and parkinsonism-dementia on Guam. *Neurology* **35**, 193–198 (1985).
20. Shimizu, F. *et al.* Cloning and chromosome assignment to 1q32 of a human cDNA (*RAB7L1*) encoding a small GTP-binding protein, a member of the RAS superfamily. *Cytogenet. Cell Genet.* **77**, 261–263 (1997).
21. Ostvold, A.C. *et al.* Molecular cloning of a mammalian nuclear phosphoprotein NUCKS, which serves as a substrate for Cdk1 *in vivo*. *Eur. J. Biochem.* **268**, 2430–2440 (2001).
22. Dixon, A.L. *et al.* A genome-wide association study of global gene expression. *Nat. Genet.* **39**, 1202–1207 (2007).
23. Yamamoto-Katayama, S. *et al.* Crystallographic studies on human BST-1/CD157 with ADP-ribosyl cyclase and NAD glycohydrolase activities. *J. Mol. Biol.* **316**, 711–723 (2002).
24. Lee, H.C. *et al.* Physiological functions of cyclic ADP-ribose and NAADP as calcium messengers. *Annu. Rev. Pharmacol. Toxicol.* **41**, 317–345 (2001).
25. Wilson, C.J. & Callaway, J.C. Coupled oscillator model of the dopaminergic neuron of the substantia nigra. *J. Neurophysiol.* **83**, 3084–3100 (2000).
26. Chan, C.S. *et al.* 'Rejuvenation' protects neurons in mouse models of Parkinson's disease. *Nature* **447**, 1081–1086 (2007).
27. Surmeier, D.J. Calcium, ageing, and neuronal vulnerability in Parkinson's disease. *Lancet Neurol.* **6**, 933–938 (2007).
28. Singleton, A.B. *et al.* α-Synuclein locus triplication causes Parkinson's disease. *Science* **302**, 841 (2003).
29. Uldry, M. *et al.* Identification of a mammalian H(+)-myo-inositol symporter expressed predominantly in the brain. *EMBO J.* **20**, 4467–4477 (2001).
30. Skipper, L. *et al.* Comprehensive evaluation of common genetic variation within *LRRK2* reveals evidence for association with sporadic Parkinson's disease. *Hum. Mol. Genet.* **14**, 3549–3556 (2005).
31. Biskup, S. *et al.* Common variants of *LRRK2* are not associated with sporadic Parkinson's disease. *Ann. Neurol.* **58**, 905–908 (2005).
32. Smith, W.W. *et al.* Kinase activity of mutant LRRK2 mediates neuronal toxicity. *Nat. Neurosci.* **9**, 1231–1233 (2006).
33. West, A.B. *et al.* Parkinson's disease-associated mutations in leucine-rich repeat kinase 2 augment kinase activity. *Proc. Natl. Acad. Sci. USA* **102**, 16842–16847 (2005).
34. Gilks, W.P. *et al.* A common *LRRK2* mutation in idiopathic Parkinson's disease. *Lancet* **365**, 415–416 (2005).
35. Hutton, M. *et al.* Association of missense and 5'-splice-site mutations in tau with the inherited dementia FTDP-17. *Nature* **393**, 702–705 (1998).
36. Pittman, A.M. *et al.* Linkage disequilibrium fine mapping and haplotype association analysis of the tau gene in progressive supranuclear palsy and corticobasal degeneration. *J. Med. Genet.* **42**, 837–846 (2005).
37. Webb, A. *et al.* Role of the tau gene region chromosome inversion in progressive supranuclear palsy, corticobasal degeneration, and related disorders. *Arch. Neurol.* **65**, 1473–1478 (2008).
38. Healy, D.G. *et al.* Tau gene and Parkinson's disease: a case-control study and meta-analysis. *J. Neurol. Neurosurg. Psychiatry* **75**, 962–965 (2004).

FEBS Letters 584 (2010) 1073–1079

ELSEVIER

FEBS Letters

journal homepage: www.FEBSLetters.org

PINK1 is recruited to mitochondria with parkin and associates with LC3 in mitophagy

Sumihiro Kawajiri [a,1], Shinji Saiki [a,1], Shigeto Sato [a], Fumiaki Sato [b], Taku Hatano [a], Hiroto Eguchi [a], Nobutaka Hattori [a,*]

[a] Department of Neurology, Juntendo University School of Medicine, 2-1-1 Hongo, Bunkyo-ku, Tokyo 113-8421, Japan
[b] Research Institute for Disease of Old Age, Juntendo University School of Medicine, 2-1-1 Hongo, Bunkyo-ku, Tokyo 113-8421, Japan

ARTICLE INFO

Article history:
Received 16 December 2009
Revised 29 January 2010
Accepted 2 February 2010
Available online 12 February 2010

Edited by Jesus Avila

Keywords:
PTEN-induced putative kinase 1
Parkin
Mitophagy
Autophagy
Parkinson's disease

ABSTRACT

Mutations in *PTEN-induced putative kinase 1 (PINK1)* cause recessive form of Parkinson's disease (PD). PINK1 acts upstream of parkin, regulating mitochondrial integrity and functions. Here, we show that PINK1 in combination with parkin results in the perinuclear mitochondrial aggregation followed by their elimination. This elimination is reduced in cells expressing PINK1 mutants with wild-type parkin. Although wild-type PINK1 localizes in aggregated mitochondria, PINK1 mutants localization remains diffuse and mitochondrial elimination is not observed. This phenomenon is not observed in autophagy-deficient cells. These results suggest that mitophagy controlled by the PINK1/parkin pathway might be associated with PD pathogenesis.

Structured summary:
MINT-7557195: *PINK1* (uniprotkb:Q9BXM7) *physically interacts* (MI:0915) with *LC3* (uniprotkb:Q9GZQ8) by *anti tag coimmunoprecipitation* (MI:0007)
MINT-7557109: *LC3* (uniprotkb:Q9GZQ8) and *PINK1* (uniprotkb:Q9BXM7) *colocalize* (MI:0403) by *fluorescence microscopy* (MI:0416)
MINT-7557121: *tom20* (uniprotkb:Q15388) and *PINK1* (uniprotkb:Q9BXM7) *colocalize* (MI:0403) by *fluorescence microscopy* (MI:0416)
MINT-7557138: *parkin* (uniprotkb:O60260), *PINK1* (uniprotkb:Q9BXM7) and *tom20* (uniprotkb:Q15388) *colocalize* (MI:0403) by *fluorescence microscopy* (MI:0416)
MINT-7557173: *LC3* (uniprotkb:Q9GZQ8) *physically interacts* (MI:0915) with *PINK1* (uniprotkb:Q9BXM7) by *anti bait coimmunoprecipitation* (MI:0006)

1. Introduction

Parkinson's disease (PD) is a neurodegenerative disease characterized by loss of dopaminergic neurons in the substantia nigra. Mitochondrial dysfunction has been proposed as a major factor in the pathogenesis of sporadic and familial PD [1. In particular, the identification of mutations in *PTEN-induced putative kinase 1 (PINK1)* has strongly implicated mitochondrial dysfunction in the pathogenesis of PD [2]. PINK1 contains an N-terminal mitochondrial targeting sequence (MTS) and a serine/threonine kinase domain [2].

Several studies have shown that PINK1 acts upstream of parkin in the same genetic pathway [3,4]. Overexpression of PINK1 promotes mitochondrial fission [5]. Fission followed by selective fusion segregates dysfunctional mitochondria and permits their removal by autophagy [6]. Parkin is associated with mitochondrial elimination in cultured cells treated with the mitochondrial uncoupler carbonyl cyanide *m*-chlorophenylhydrazone (CCCP) [7], but little is known about the biological function of PINK1 in this context. Likewise, although co-overexpressed both PINK1 and parkin colocalized with mitochondria [8] and are associated with mitochondrial autophagy (mitophagy) [9], the exact mechanism of the mitochondrial elimination via autophagy has not been examined.

Here, we describe the characterization of mitophagy induced by co-overexpressing both proteins and report that the phenomenon is dependent on PINK1 kinase activity and mitochondrial localization.

Abbreviations: CCCP, carbonyl cyanide *m*-chlorophenylhydrazone; 3-MA, 3-methyladenine; MEFs, mouse embryonic fibroblasts; MTS, mitochondrial targeting sequence; PD, Parkinson's disease; PINK1, PTEN-induced putative kinase 1; UPS, ubiquitin–proteasome system

* Corresponding author. Address: Department of Neurology, Juntendo University School of Medicine, 2-1-1 Hongo, Bunkyo-ku, Tokyo, 113-8421, Japan. Fax: +81 3 5800 0547.
E-mail address: nhattori@juntendo.ac.jp (N. Hattori).
[1] Joint first authors.

0014-5793/$36.00
doi:10.1016/j.febslet.2010.02.016

Furthermore, we found that PINK1 interacts with LC3–phospholipid conjugate (LC3-II), a well established marker for autophagosomes [10]. These results provide novel insights into the pathogenesis of PD.

2. Materials and methods

2.1. Antibodies

Anti-FLAG antibodies (M2, polyclonal) and anti-LC3B antibody (rabbit) were obtained from Sigma. Anti-actin antibody (mouse) was from Millipore. Anti-Tom20 antibody (rabbit) was from Santa Cruz Biotechnology. Anti-LDH antibody (goat) was from Abcam. Anti-LC3 antibody (rabbit) was from MBL. Secondary antibodies, conjugated to horseradish peroxidase, were from GE HealthCare Bio-Sciences and Alexa Fluor 488, 546, 594, and 647 conjugated secondary antibodies were from Invitrogen-Molecular Probes.

2.2. Plasmids

A cDNA encoding wild-type PINK1 was amplified with appropriate primers and ligated into the BamHI sites of the (C-terminal tagged) 3xFLAG pCMV-10™ expression plasmid (Sigma). Mutations in PINK1 were introduced by site-directed mutagenesis (Stratagene) according to manufacturer's instructions. GFP-parkin was subcloned into pcDNA3.1 (Invitrogen).

2.3. Cell culture

HeLa, HEK293 cells and Atg7$^{+/+}$ and $^{-/-}$ mouse embryonic fibroblasts (MEFs) (a gift from Dr. Komatsu) were grown in DMEM (Sigma) supplemented with 10% FBS (Sigma) and 1% penicillin–streptomycin (Invitrogen) at 37 °C and 5% CO_2. For pharmacological studies, E64d, pepstatin A, rapamycin, 3-MA, and CCCP (Sigma) were added at indicated times and concentrations.

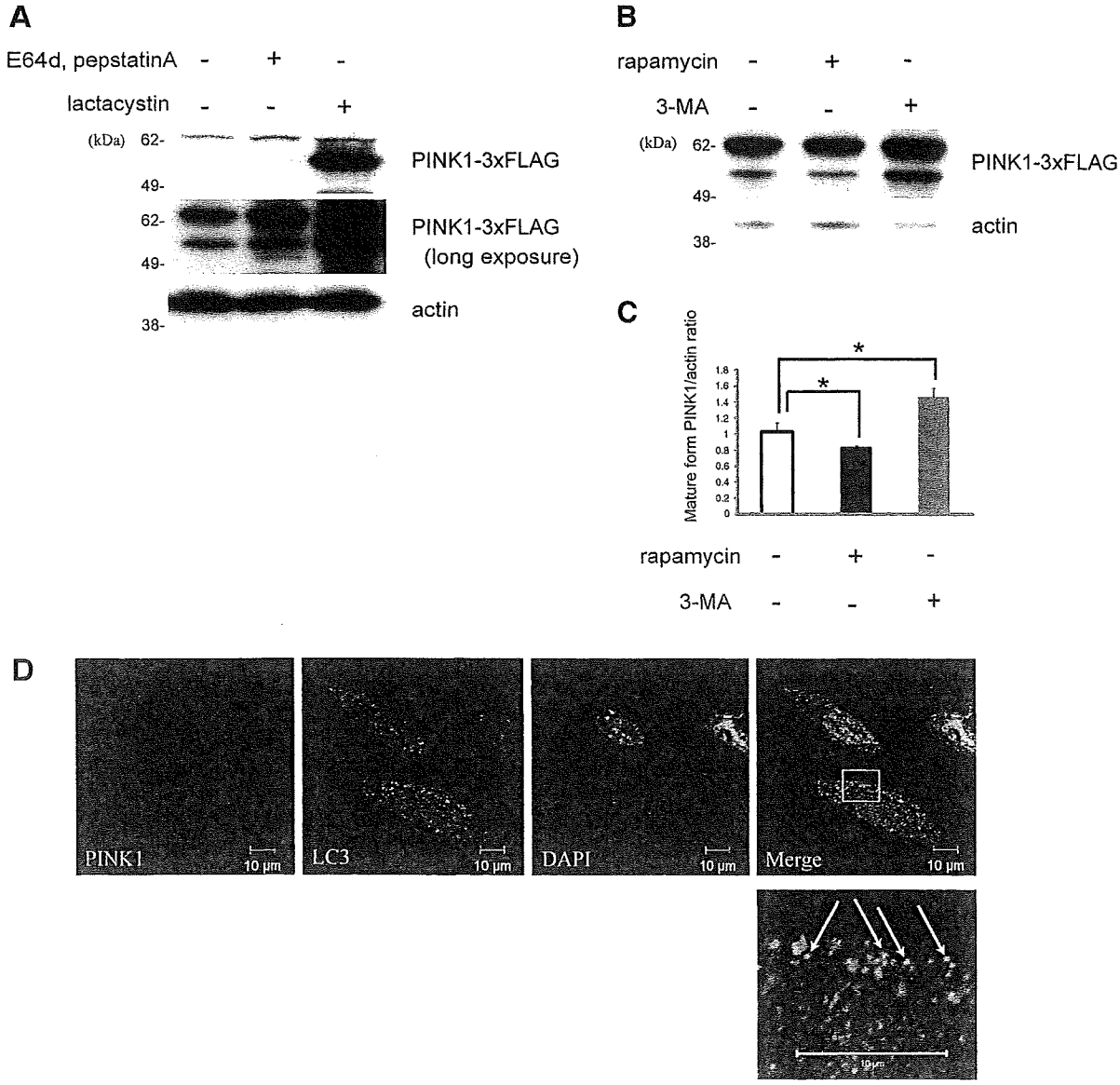

Fig. 1. PINK1 is degraded by autophagy as well as by the ubiquitin–proteasome system. (A and B) PINK1 levels in HEK293 cells stably expressing PINK1-3xFLAG treated or untreated with E64d (10 μg/ml) + pepstatin A (10 μg/ml) or lactacystin (10 μM) (A), and 3-MA (10 mM) or rapamycin (200 nM) (B), for 24 h were analyzed by immunoblotting with anti-FLAG antibodies (M2). The bottom panels show actin as loading control. (C) Quantification of (B); $^{*}P < 0.05$. Error bars indicate standard deviation of at least three experiments. (D) Immunocytochemistry of HeLa cells transiently overexpressing PINK1-3xFLAG, 24 h after transfection. PINK1 or LC3 are in red or green, respectively. The boxed area is shown in the bottom image at a higher magnification. Bars, 10 μM.

2.4. Cell transfection and establishment of stable cell lines

Cells were transfected with the indicated plasmids using Lipofectamine 2000 (Invitrogen) and Lipofectamine LTX with PLUS Reagent (Invitrogen) according to manufacturer's instructions. For stable overexpression of PINK1, HEK293 cells were transfected with PINK1 plasmids and then selected using G418.

2.5. Immunocytochemistry

Cells were fixed with 4% paraformaldehyde, permeabilized with 1× PBS containing 0.5% Triton X-100, and incubated in PBS containing 10% FBS and 1% BSA. Cells were then incubated overnight with primary antibodies, followed by incubation with secondary antibodies for 1 h. Cells were then mounted with Vectashield containing DAPI (Vector Laboratories). Cells were visualized using a ZEISS LSM510 confocal microscope.

2.6. Cell fractionation

Cells were fractionated using the mitochondrial isolation kit for cultured cells (Pierce) according to manufacturer's instructions.

2.7. Immunoprecipitation and immunoblotting

Cells were lysed on ice in lysis buffer [10 mM Tris–HCl (pH 7.5), 150 mM NaCl, 1 mM EDTA, 1% NP-40, and protease inhibitors (complete, Mini, EDTA-free, (Roche Applied Science))]. Cell lysates were immunoprecipitated using Dynabeads protein G (Invitrogen) according to manufacturer's instructions and immunoblotting was performed previously described elsewhere [11].

3. Results and discussion

3.1. PINK1 is degraded by autophagy as well as by the ubiquitin–proteasome system (UPS)

Previous studies have shown that PINK1 is degraded by the UPS [12], but it remains unclear whether autophagy also affects its degradation. We, therefore, tested whether PINK1 could be degraded via the UPS and/or autophagy, using HEK293 cells stably expressing PINK1-3xFLAG. Immunoblot analysis identifies PINK1 in two bands. The upper band represents full-length PINK1 (~66 kDa), whereas the lower band represents the mature form of PINK1 (~55 kDa), in which the MTS has been removed [13,14]. As others

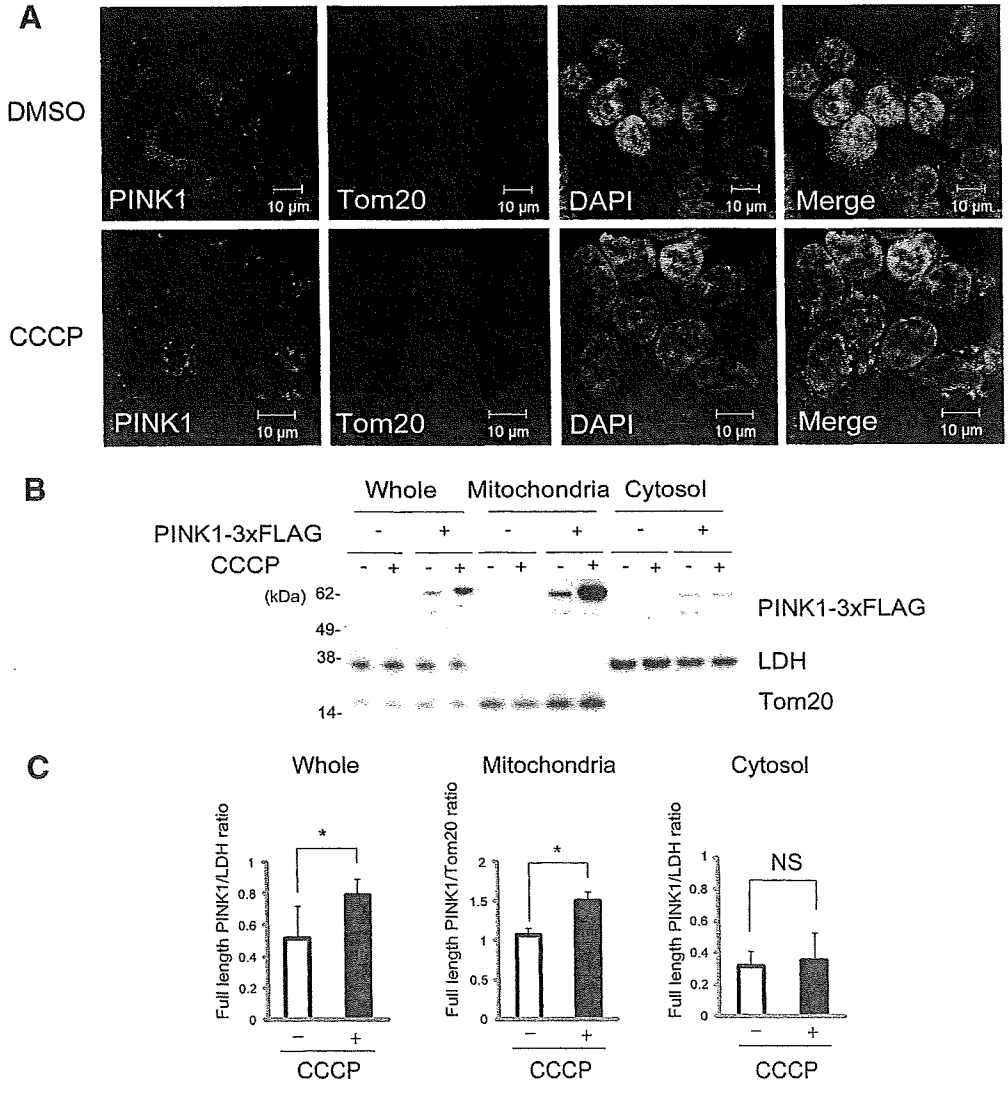

Fig. 2. PINK1 is recruited to depolarized mitochondria. (A) Immunocytochemistry of HEK293 cells stably expressing PINK1-3xFLAG treated with DMSO or CCCP (10 μM) for 3 h. PINK1 or Tom20 are in green or red, respectively. Bars, 10 μM. (B) HEK293 cells stably expressing 3xFLAG-empty vector or PINK1-3xFLAG treated with DMSO or CCCP (10 μM) for 3 h were fractionated and immunoblotted for FLAG, Tom20, and LDH. (C) Quantification of (B); $^*P < 0.05$. NS, non-significant. Error bars indicate standard deviation of at least three experiments.

have shown [12], levels of mature form PINK1 were increased by treatment with a proteasome inhibitor (lactacystin) (Fig. 1A). Also, they were increased by lysosome protease inhibitors (E64d + pepstatin A), which block autophagic flux (Fig. 1A). Next, we investigated the effects of other autophagy modulators (rapamycin and 3-methyladenine (3-MA)) on levels of PINK1. As expected, rapamycin treatment decreased mature form PINK1 levels, although 3-MA treatment increased them (Fig. 1B and C). Immunocytochemistry of HeLa cells transiently overexpressing PINK1-3xFLAG demonstrated partial colocalization of PINK1 with endogenous LC3 (an autophagosomal marker) (Fig. 1D). These data suggested that PINK1 is degraded via autophagy as well as by the UPS.

3.2. PINK1 is recruited to depolarized mitochondria

In cultured cells treated with CCCP, parkin is selectively recruited to degraded mitochondria and promotes mitophagy [7]. PINK1 and parkin function in the same genetic pathway to regulate mitochondrial integrity [3,4]. To investigate the interaction between depolarized mitochondria and PINK1, we tested for a change of PINK1 localization following treatment with CCCP. In HEK293 cells stably expressing PINK1, mitochondria stained with antibody against Tom20, a receptor protein of the mitochondrial outer membrane, were aggregated around the nucleus and fragmented and showed marked accumulation of PINK1 (Fig. 2A). The mitochondrial translocation of PINK1, caused by CCCP, was also assayed by immunoblotting. Levels of full-length PINK1 in the mitochondrial fraction were increased by CCCP treatment (Fig. 2B and C).

3.3. Mitochondrial elimination is accomplished by overexpression of wild-type PINK1 in combination with parkin

PINK1 has been reported to promote parkin translocation to mitochondria [8]. To further investigate the molecular interaction between PINK1 and parkin, the following experiments with HeLa cells overexpressing both PINK1 and parkin were performed. Twenty-four hours after transfection, mitochondrial aggregation and recruitment of PINK1 and parkin to the aggregated mitochondria were observed only in cells positive for GFP-parkin and PINK1-3xFLAG. Moreover, parkin completely colocalized with aggregated mitochondria (Fig. 3A and B). Partial colocalization of wild-type PINK1 with parkin has been previously reported in cells overexpressing both PINK1 and parkin; however, the association with mitochondria was not examined [15]. Also, parkin colocalization with PINK1 in aggregated mitochondria has been previously reported [8]. To confirm the exact effect of both PINK1 and parkin on mitochondria, we examined the fate of the degraded mitochondria, 48 h after transfection. In cells overexpressing both PINK1 and parkin, the mitochondria were completely absent, while mitochondria were still present in cells overexpressing either PINK1 or parkin (Fig. 3C). These data indicate that both PINK1 and parkin might be indispensable for mitochondrial elimination.

3.4. PINK1 mutants remain diffusely distributed and are not recruited to mitochondria, resulting in reduced mitochondrial elimination

PD-associated mutations in PINK1 have been found in both the kinase and C-terminal domains [2,16]. Among these mutations, G309D, L347P, and G409V are expected to cause a reduction in the kinase activity of PINK1 [13,14,17]. Therefore, we generated PINK1 mutants with G309D, L347P and G409V and two deletion mutants without the MTS (ΔN: deleted amino acids 156–581 and KD: deleted amino acids 156–509) and performed similar transfection experiments to those described above. Neither recruitment of parkin and/or mutant PINK1 to the mitochondria nor mitochondrial aggregation was detected 24 h after transfection (data not shown). Forty-eight hours after transfection, the G309D/L347P/G409V mutants preserved their mitochondrial localization, whilst less mitochondrial elimination was detected compared with those cells expressing both wild-type PINK1 and parkin. The ΔN/KD mutants were diffusely distributed without apparent colocalization to the mitochondria and no mitochondrial elimination was observed (Fig. 4A–C). Also, we confirmed mitochondrial elimination by immunoblotting. Levels of Tom20 were decreased in cells expressing both parkin and wild-type PINK1 but not in the cells expressing PINK1 mutants (Fig. 4D and E). These findings suggested that the

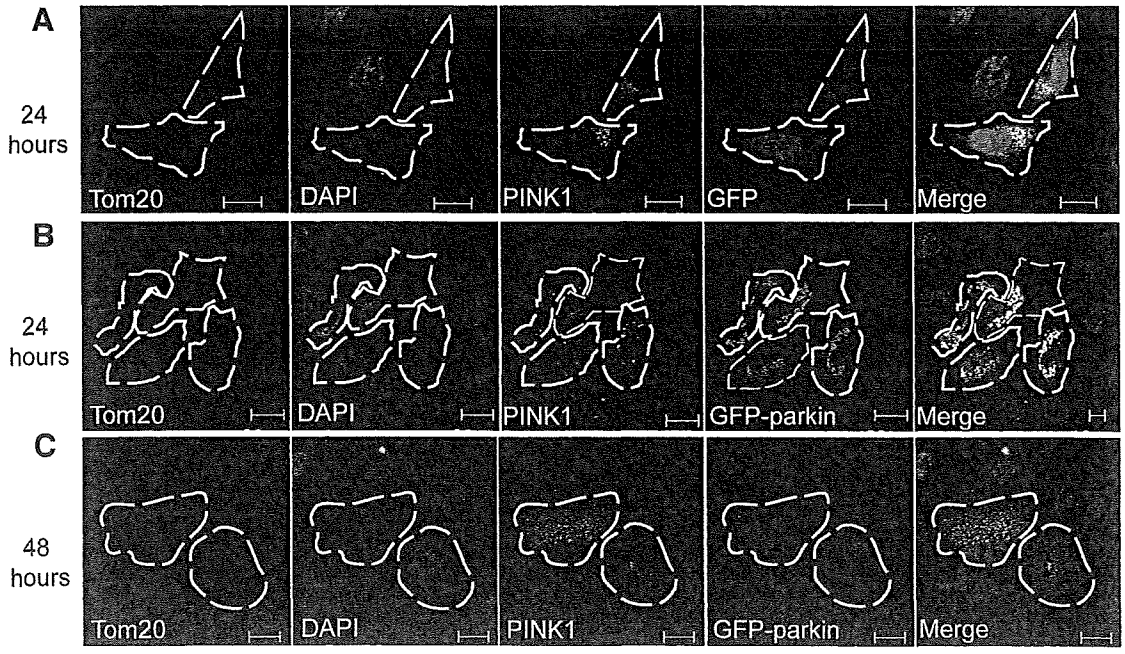

Fig. 3. Mitochondrial elimination is accomplished by overexpression of wild-type PINK1 in combination with parkin. (A and B) Immunocytochemistry of HeLa cells 24 h after transient co-overexpression of wild-type PINK1-3xFLAG (PINK1-WT) and GFP-empty vector (GFP) (A) or GFP-parkin (B) and 48 h after transient co-overexpression of PINK1-WT and GFP-parkin (C). Tom20, wild-type PINK1, or GFP are red, white, or green, respectively. Bars, 10 μm.

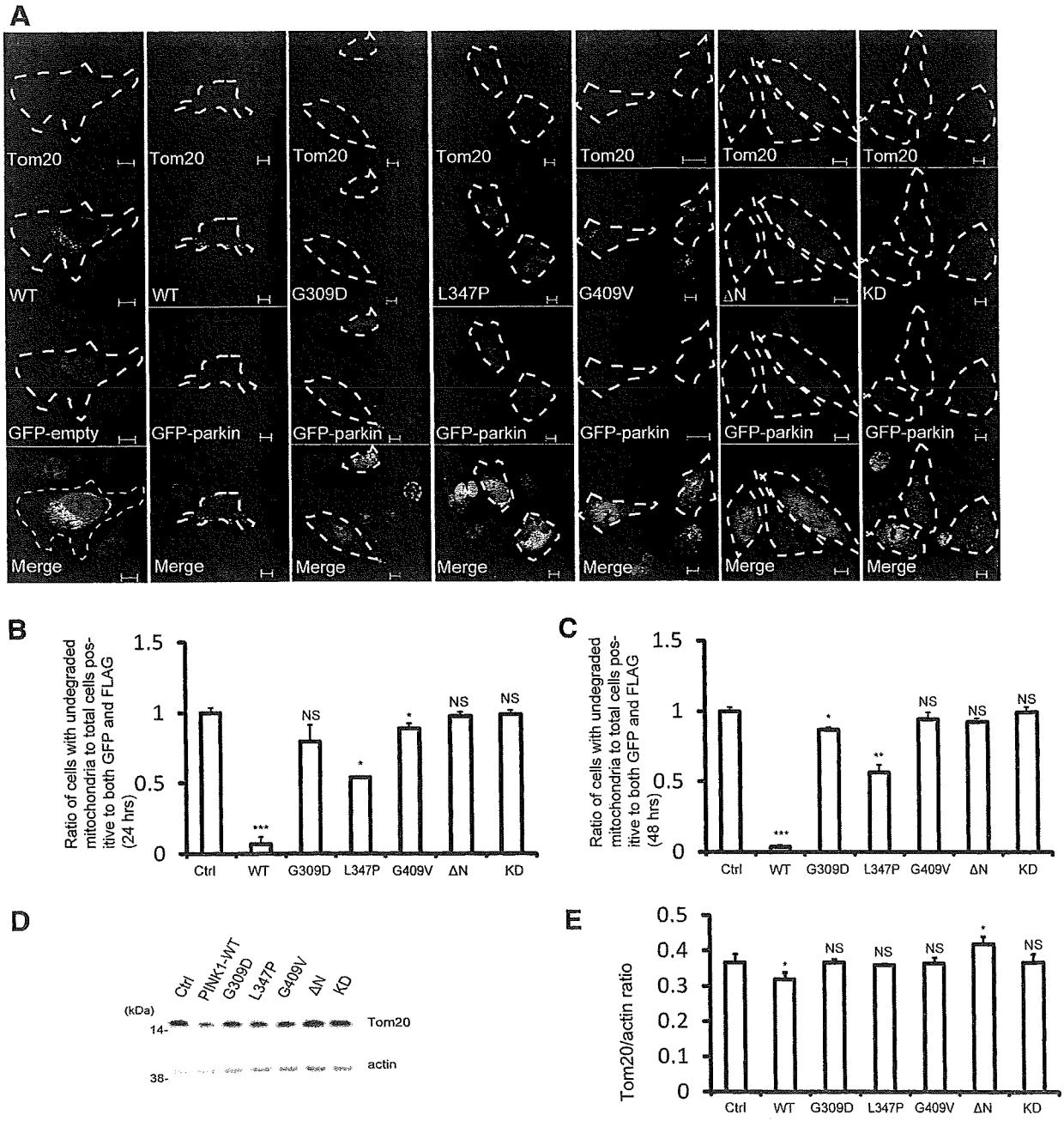

Fig. 4. PINK1 mutants remain diffusely distributed and are not recruited to mitochondria, resulting in reduced mitochondrial elimination. (A) Immunocytochemistry of HeLa cells transiently overexpressing GFP-empty vector and PINK1-3xFLAG (WT) as control, and GFP-parkin and PINK1-3xFLAG (WT or various mutants), 48 h after transfection. Tom20, WT and PINK1 mutants, or GFP are in red, white, or green, respectively. Bars, 10 μm. (B and C) Ratio of cells with undegraded mitochondria to total cells positive for both GFP and FLAG, 24 h (B) and 48 h (C) after transfection are shown in the graph. (D) Levels of Tom20 in HeLa cells transiently overexpressing GFP-empty vector and PINK1-3xFLAG (WT), and GFP-parkin and PINK1-3xFLAG (WT or various mutants) were analyzed with immunoblotting. (E) Quantification of (D); error bars indicate standard deviation of at least three experiments. $^{*}P < 0.05$, $^{**}P < 0.01$, $^{***}P < 0.001$. NS, non-significant.

kinase activity and mitochondrial localization of PINK1 are indispensable for mitochondrial elimination.

3.5. Overexpression of wild-type PINK1 in combination with parkin induces mitophagy

Very recently, it has been reported aggregated mitochondria in cells overexpressing both PINK1 and parkin colocalize with lysosomes as well as autophagosomes [9]. However, the fate of perinuclear aggregated mitochondria has not been examined. Therefore, we checked whether PINK1–parkin dependent mitochondrial elimination was dependent on mitophagy. Mitochondrial elimination was enhanced by overexpression of PINK1 with parkin in wild-type MEFs. On the other hand, Atg7$^{-/-}$ MEFs, which lack a key component of the autophagy system, retain expression of Tom20 (Fig. 5A and B). To further analyze this hypothesis, we examined the change of endogenous LC3 distribution following both PINK1 and parkin overexpression. We confirmed accumulation of parkin, which overlaps with aggregated mitochondria (refer to Fig. 3), in cells expressing both wild-type proteins. Likewise, endogenous LC3 mainly colocalized with wild-type PINK1, adjoined to the outer mitochondrial membrane, but did not colocalize with G409V or ΔN

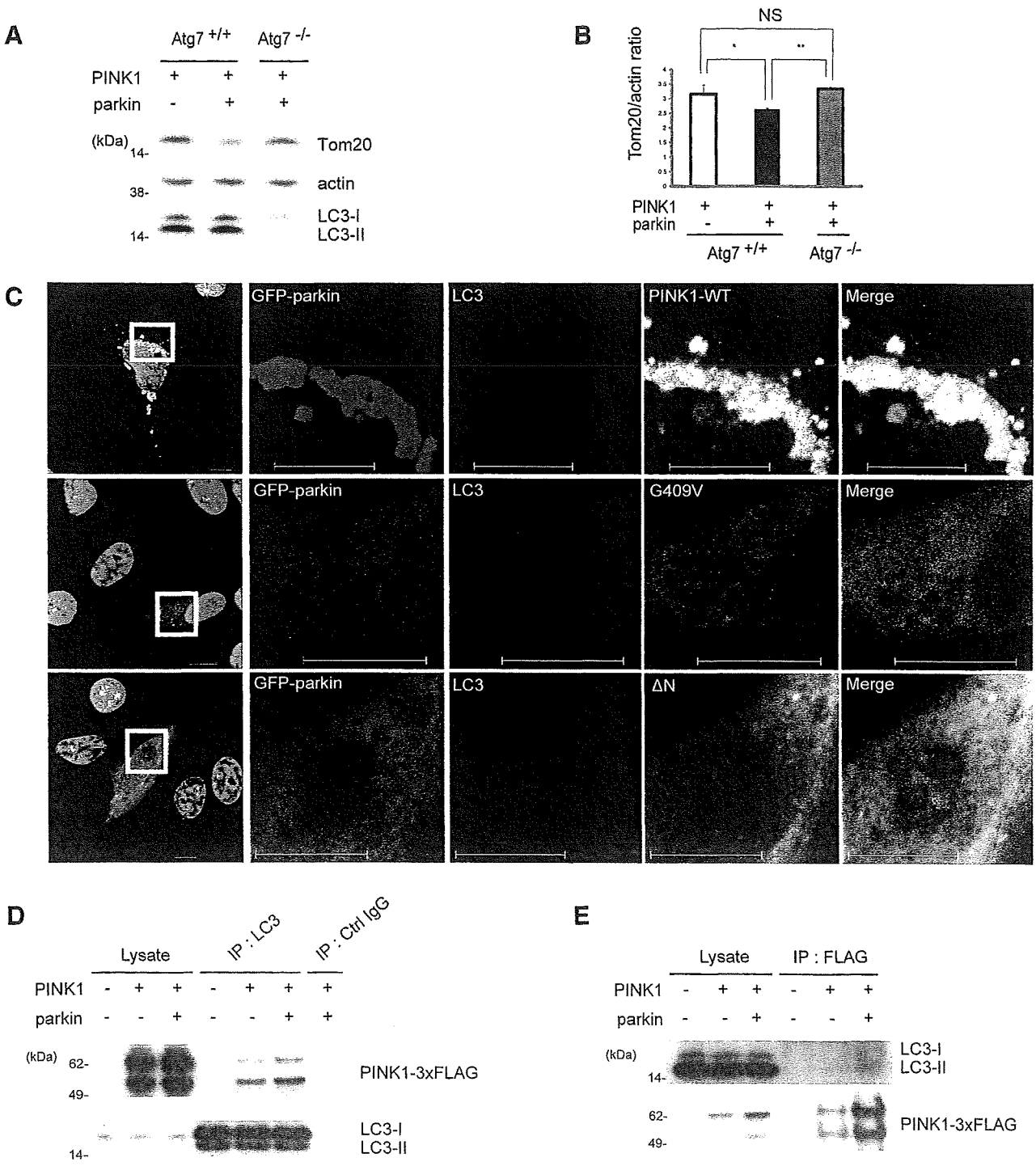

Fig. 5. Overexpression of wild-type PINK1 in combination with parkin induces mitophagy. (A) Levels of Tom20 in Atg7$^{+/+}$ MEFs overexpressing GFP-empty vector and PINK1-3xFLAG and those in Atg7$^{+/+}$ and Atg7$^{-/-}$ MEFs overexpressing GFP-parkin and PINK1-3xFLAG, 48 h after transfection were analyzed by immunoblotting. (B) Quantification of (A); error bars indicate standard deviation of at least three experiments. $^{*}P < 0.05$, $^{**}P < 0.01$, NS, non-significant. (C) Immunocytochemistry of HeLa cells transiently overexpressing GFP-parkin and PINK1-3xFLAG (wild-type, G409V, and ΔN), 24 h after transfection. PINK1 (WT and mutants), LC3, or GFP-parkin are in white, red, or green, respectively. The boxed areas are shown in the three right-hand images at a higher magnification. Bars, 10 μm. (D and E) HeLa cells overexpressing 3xFLAG-empty vector and GFP-empty vector, PINK1-3xFLAG and GFP-empty vector, or PINK1-3xFLAG and GFP-parkin, 24 h after transfection were immunoprecipitated with anti-LC3 antibodies (D) or anti-FLAG antibodies (E) and immunoblotted for FLAG or LC3. Immunoblotting of total lysates was performed to test the expression levels. IP, immunoprecipitation.

(Fig. 5C), nor with G309D, L347P and KD (data not shown). LC3 also partially colocalized with parkin. Compared with Fig. 1D, the colocalization of endogenous LC3 with PINK1 was markedly enhanced. Next, to investigate direct interaction, cell lysates were immunoprecipitated using anti-LC3 antibodies and immunoblotted with anti-FLAG antibodies (Fig. 5D). The reverse immunoprecipitation was also performed (Fig. 5E). These results allowed us to conclude that PINK1 binds with LC3-II. Taken together, we concluded that mitochondrial elimination by the PINK1–parkin pathway is dependent on mitochondrial autophagic activity.

In this study, we have found that overexpression of both proteins enhances mitochondrial elimination via autophagy. In

contrast to the results of a *Drosophila* study, a PINK1–parkin pathway promotes mitochondrial enlargement or aggregation in mammalian cellular models [8,18]. However, only PINK1 overexpressing cells exhibit longer mitochondria with increased interconnectivity, but the abnormal mitochondria do not elicit an autophagic response [12]. Consistent with this, wild-type PINK1 overexpression did not change the level of endogenous LC3-II (data not shown). Therefore, coordinating activation of parkin and PINK1 contributes to mitophagy.

PINK1 localization in mitochondria is dependent on its MTS region and it exhibits autophosphorylation activity in vitro [2,13,14]. Parkin is recognized as an in vivo substrate of PINK1 and parkin site-direct phosphorylation by wild-type PINK1 is critical for the translocation of parkin into the mitochondria in cellular and *Drosophila* models [8]. In agreement with this report, our study showed that parkin recruitment to the mitochondria by PINK1 was dependent on PINK1 kinase activity.

Silencing of PINK1 with shRNA increased mitochondrial fission and induced mitophagy [12]. Although PINK1 overexpression is protective against oxidative stress-induced apoptotic cell death [2,19,20], excess wild-type PINK1 without parkin overexpression does not elicit mitochondrial autophagy [12]. Our immunocytochemical experiments revealed that PINK1 co-overexpressed with parkin colocalized mainly with LC3-positive vesicles and partially with perinuclear aggregated mitochondria, which were expected to colocalize with aggregated parkin. In addition, molecular binding between PINK1 and LC3-II was confirmed by immunoprecipitation, which suggests that association between PINK1 and LC3 contribute to mitophagy. Combined with the observation by Vives-Bausa et al., although it is not clear whether an excess of mitophagy would be harmful to cells, a PINK1–parkin pathway, which is regulated by kinase activity and/or the mitochondrial localization of PINK1, would control mitochondrial maintenance via the autophagic machinery.

Acknowledgments

We thank Drs. Masaaki Komatsu and Yu-shin Sou (Laboratory of Frontier Science, Tokyo Metropolitan Institute of Medical Science) for providing Atg7$^{-/-}$ MEFs and Hattori's laboratory members for helpful discussions. We are grateful to Drs. Junichi Nakamoto, Yoko Imamichi, and Akiko Egashira for technical assistance. This study was supported by a Young Scientist Grant (F.S. and S. Saiki), an All Japan Coffee Association Grant (S. Saiki), a Takeda Scientific Association Grant (S. Saiki) and a Grant from Nagao Memorial Fund (S. Saiki).

References

[1] Abou-Sleiman, P.M., Muqit, M.M. and Wood, N.W. (2006) Expanding insights of mitochondrial dysfunction in Parkinson's disease. Nat. Rev. Neurosci. 7, 207–219.
[2] Valente, E.M. et al. (2004) Hereditary early-onset Parkinson's disease caused by mutations in PINK1. Science 304, 1158–1160.
[3] Clark, I.E. et al. (2006) Drosophila pink1 is required for mitochondrial function and interacts genetically with parkin. Nature 441, 1162–1166.
[4] Park, J. et al. (2006) Mitochondrial dysfunction in Drosophila PINK1 mutants is complemented by parkin. Nature 441, 1157–1161.
[5] Yang, Y., Ouyang, Y., Yang, L., Beal, M.F., McQuibban, A., Vogel, H. and Lu, B. (2008) Pink1 regulates mitochondrial dynamics through interaction with the fission/fusion machinery. Proc. Natl. Acad. Sci. USA 105, 7070–7075.
[6] Twig, G. et al. (2008) Fission and selective fusion govern mitochondrial segregation and elimination by autophagy. EMBO J. 27, 433–446.
[7] Narendra, D., Tanaka, A., Suen, D.F. and Youle, R.J. (2008) Parkin is recruited selectively to impaired mitochondria and promotes their autophagy. J. Cell Biol. 183, 795–803.
[8] Kim, Y. et al. (2008) PINK1 controls mitochondrial localization of Parkin through direct phosphorylation. Biochem. Biophys. Res. Commun. 377, 975–980.
[9] Vives-Bauza, C. et al. (2010) PINK1-dependent recruitment of Parkin to mitochondria in mitophagy. Proc. Natl. Acad. Sci. USA 107, 378–383.
[10] Kabeya, Y. et al. (2000) LC3, a mammalian homologue of yeast Apg8p, is localized in autophagosome membranes after processing. EMBO J. 19, 5720–5728.
[11] Hatano, T., Kubo, S., Imai, S., Maeda, M., Ishikawa, K., Mizuno, Y. and Hattori, N. (2007) Leucine-rich repeat kinase 2 associates with lipid rafts. Hum. Mol. Genet. 16, 678–690.
[12] Dagda, R.K., Cherra 3rd, S.J., Kulich, S.M., Tandon, A., Park, D. and Chu, C.T. (2009) Loss of PINK1 function promotes mitophagy through effects on oxidative stress and mitochondrial fission. J. Biol. Chem. 284, 13843–13855.
[13] Silvestri, L., Caputo, V., Bellacchio, E., Atorino, L., Dallapiccola, B., Valente, E.M. and Casari, G. (2005) Mitochondrial import and enzymatic activity of PINK1 mutants associated to recessive parkinsonism. Hum. Mol. Genet. 14, 3477–3492.
[14] Beilina, A., Van Der Brug, M., Ahmad, R., Kesavapany, S., Miller, D.W., Petsko, G.A. and Cookson, M.R. (2005) Mutations in PTEN-induced putative kinase 1 associated with recessive parkinsonism have differential effects on protein stability. Proc. Natl. Acad. Sci. USA 102, 5703–5708.
[15] Um, J.W., Stichel-Gunkel, C., Lubbert, H., Lee, G. and Chung, K.C. (2009) Molecular interaction between parkin and PINK1 in mammalian neuronal cells. Mol. Cell Neurosci. 40, 421–432.
[16] Hatano, Y. et al. (2004) Novel PINK1 mutations in early-onset parkinsonism. Ann. Neurol. 56, 424–427.
[17] Sim, C.H., Lio, D.S., Mok, S.S., Masters, C.L., Hill, A.F., Culvenor, J.G. and Cheng, H.C. (2006) C-terminal truncation and Parkinson's disease-associated mutations down-regulate the protein serine/threonine kinase activity of PTEN-induced kinase-1. Hum. Mol. Genet. 15, 3251–3262.
[18] Exner, N. et al. (2007) Loss-of-function of human PINK1 results in mitochondrial pathology and can be rescued by parkin. J. Neurosci. 27, 12413–12418.
[19] Petit, A. et al. (2005) Wild-type PINK1 prevents basal and induced neuronal apoptosis, a protective effect abrogated by Parkinson disease-related mutations. J. Biol. Chem. 280, 34025–34032.
[20] Pridgeon, J.W., Olzmann, J.A., Chin, L.S. and Li, L. (2007) PINK1 protects against oxidative stress by phosphorylating mitochondrial chaperone TRAP1. PLoS Biol. 5, e172.